Received: 29 February 2024 | Revised: 21 June 2024 | Accepted: 14 August 2024

DOI: 10.1002/joc.8607

RESEARCH ARTICLE

International Journal of Climatology RMetS

A comparative analysis of temperature trends at Modena Geophysical Observatory and Mount Cimone Observatory, Italy

Sofia Costanzini[1] | **Mauro Boccolari**[1] | **Stephanie Vega Parra**[2] | **Francesca Despini**[1] | **Luca Lombroso**[1] | **Sergio Teggi**[1]

[1]University of Modena and Reggio Emilia, Modena, Italy

[2]PhD in Sustainable Development and Climate Change, IUSS Pavia School, Pavia, Italy

Correspondence
Sofia Costanzini, University of Modena and Reggio Emilia, Via Università 4, 41121 Modena, Italy.
Email: sofia.costanzini@unimore.it

Abstract

Global warming has become a critical environmental, social, and economic threat, with increasing frequency and intensity of extreme weather events. This study aims to analyse temperature trends and climate indices in the Po Valley, a significant economic and agricultural region in Italy, by examining data from two historical stations: the urban Modena Observatory and the rural Mount Cimone Observatory. The analysis extends previous studies to 2018, assessing the magnitude of climate changes since the 1950s and isolating the Urban Heat Island (UHI) effect in Modena. Significant warming trends were confirmed at both sites, with in maximum (TX) and minimum (TN) temperatures trends nearly doubling from 1981 to 2018 compared to 1951–2018. For example, TX trends reached 0.84°C·decade^{-1} in Modena and 0.62°C·decade^{-1} at Mount Cimone, while TN trends were 0.77 and 0.80°C·decade^{-1}, respectively. Extreme climate indices showed a substantial increase in warm days and nights (TX90p and TN90p, respectively). Particularly we found TX90p of 27.5 days·decade^{-1} in Modena and 15 days·decade^{-1} at Mount Cimone while TN90p of 29.5 days·decade^{-1} in Modena, 22 days·decade^{-1} at Mount Cimone. The UHI effect significantly impacts Modena's temperature trends. Urbanization contributes up to 65% of the rise in warm nights. Specifically, frost days decreased by 1.88 days·decade^{-1} (37% of Urban Contribute, UC), tropical nights increased by 5.16 days·decade^{-1} (57% UC), warm nights increased by 12.7 days·decade^{-1} (65% UC), and cool nights decreased by 3.19 days·decade^{-1} (39% UC). Overall, the study underscores the importance of considering both global and local factors in regional climate trend analysis.

KEYWORDS

Apennines, climate change, climate extremes, global warming, Po Valley, UHI, Urban Heath Island

1 | INTRODUCTION

Global warming has become increasingly apparent since the last decades of the previous century, posing an environmental, social, and economic threat to the planet due to its widespread and intensifying effects.

Several studies in scientific literature have found that global warming is increasing the frequency of extreme weather events, including heatwaves, intense precipitation, floods, and droughts (Planton et al., 2008; Stott, 2016; Xie et al., 2015). Regarding Europe, heat waves in recent decades, especially in 2003, have had unprecedented impacts, causing significant social, economic, and environmental damage (Della-Marta et al., 2007a, 2007b; Klein Tank et al., 2005; Luterbacher et al., 2004). In Italy, temperature trends analysed over various regions show a consistent upward trend, with notable increases in recent decades (Scorzini & Leopardi, 2019; Toreti et al., 2010; Ventura et al., 2002). Researchers have also used extreme indices like the Diurnal Temperature Range (DTR) to study climate patterns, highlighting a reduction in temperature ranges due to more significant increases in minimum temperatures (Bartolini et al., 2008; Brunetti et al., 2000).

The Expert Team on Climate Change Detection and Indices (ETCCDI) (Klein Tank et al., 2009) has identified a set of 27 climate indices crucial for analysing temperature and precipitation, with a specific focus on extreme characteristics (Chervenkov & Slavov, 2021; Kang et al., 2014; Klein Tank et al., 2005; Meehl et al., 2000; Sillmann et al., 2013a, 2013b).

The present study fits within this context, aiming to analyse temperature trends and ETCCDI indices to estimate local climate change. The area considered is the Po Valley, which hosts a third of Italy's population. This territory has been experiencing increased economic and agricultural vulnerability due to the rise in annual temperatures from the mid-20th century to the present with significant impacts on crop production and in the industrial/civil sector (i.e., increased cooling demands for systems) (Tomozeiu et al., 2006; Zullo et al., 2019).

Thus, the paper aims to assess both the magnitude of the climate changes experienced by the territory since the 1950s and to isolate the signal of urbanization in the temperature series to understand its contribution to global warming, as done by Zhang et al. (2021).

For this purpose, we consider two historical stations with a long-standing tradition of measuring and recording meteorological parameters located in the same geographic region (Emilia Romagna region, northern Italy) but with distinct characteristics. The first station is the Geophysical Observatory of the University of Modena and Reggio Emilia (hereafter Modena Observatory), established in 1826 within the city centre of Modena in the Po Valley, an area that has experienced considerable urban development. The second station is the Mount Cimone Observatory (hereafter Cimone Observatory), an historical station of the Italian Air Force Meteorological Service. This observatory, located at an elevated position of 2165 m a.s.l. on Mount Cimone, has been collecting data since 1947. It resides in the free troposphere, free from urban influences (Carbone et al., 2014; Ramponi, 2023).

This study starts evaluating climate changes in the two locations extending the analysis of Boccolari and Malmusi (2013) to 2018 for Modena, and also includes an assessment of climate changes at Mount Cimone. It also incorporates insights from Cundari and Colombo (1992), who correlated temperature data from the Cimone Observatory with a large area in the Po Valley, demonstrating its utility for long-term temperature representation. Despite extensive use of the Cimone Observatory for CO_2 and pollution studies (Alemanno et al., 2014; Bonasoni et al., 1995, 2002; Cristofanelli et al., 2018; Fratticioli et al., 2023), there is a gap in the literature on its meteorological data since Colombo's study.

Finally, we analysed the potential contribution of urbanization to the temperature trends at the Modena Observatory station. The expansion of built-up areas near the station over time could have caused temperature increases attributable not to global warming but to the Urban Heat Island (UHI) effect (Barbieri et al., 2018; Costanzini et al., 2022). To assess the impact of the UHI, auxiliary data from the ERACLITO databases were utilized (Antolini et al., 2016). This comprehensive approach ensures that the observed temperature trends can be accurately attributed, distinguishing between global climate change and local urban influences.

2 | STUDY AREA AND DATASETS

This section outlines the data sources employed in the study, focusing on the two distinct weather stations of Modena Observatory and Cimone Observatory shown in Figure 1. Both stations play crucial roles in assessing climate changes and offer unique insights due to their disparate locations.

2.1 | Meteorological stations

2.1.1 | Modena Observatory

The Modena Observatory is housed in the East Tower of the Ducal Palace in Modena's city centre (44°38′52.59″N, 10°55′47.22″E WGS84, at 34.6 m a.s.l.). The meteorological

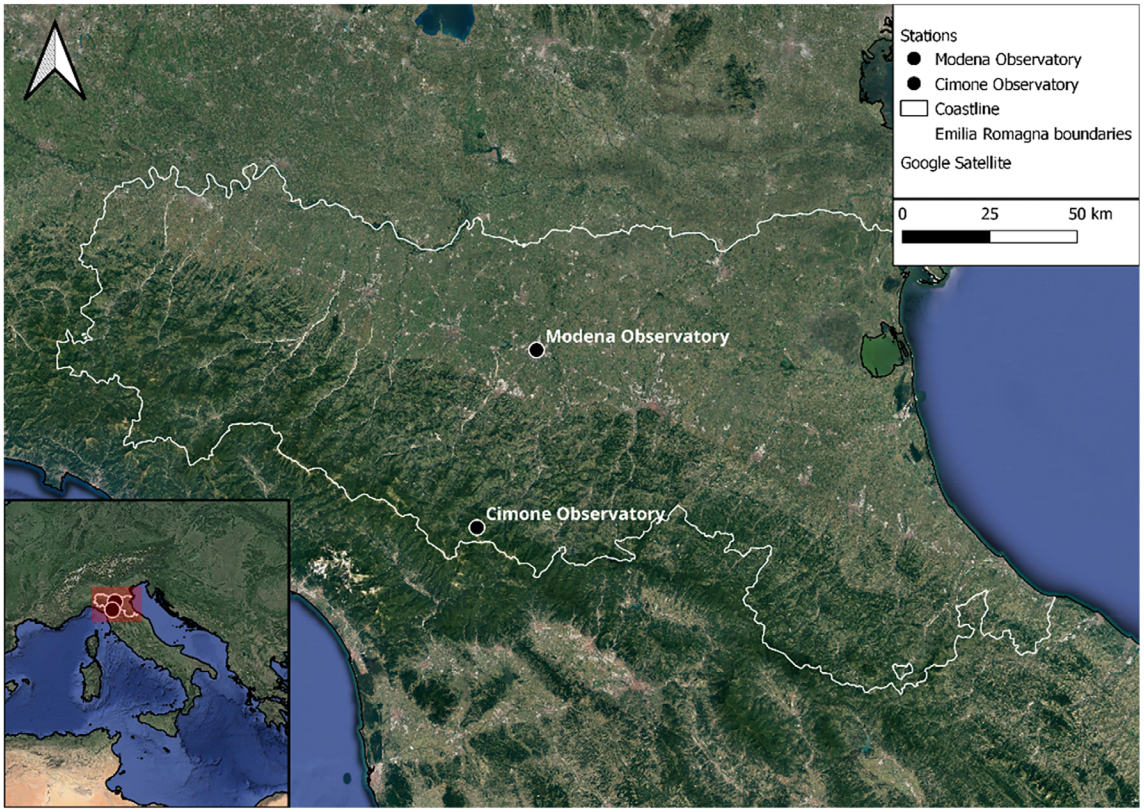

FIGURE 1 Location of the Modena Observatory within the Po Valley, north of Italy, and the Monte Cimone Observatory in the Apennines. [Colour figure can be viewed at wileyonlinelibrary.com]

instruments are located on a historic balcony, positioned at a barometric height of 64.2 m a.s.l. Established in 1826 by Francesco IV, Duke of Modena, the observatory began collecting meteorological data in 1827, encompassing parameters such as temperature, humidity, precipitation, pressure, wind speed and direction, and cloud cover. Past temperature records are comparable with present ones since 1861, marking the construction of the first meteorological window, later replaced by the historical balcony. Recognized as a Centennial Observing Station by the World Meteorological Organization (WMO), Modena Observatory attests to its longstanding commitment to meteorological observations (Lombroso et al., 2020; World Meteorological Organization, 2022).

The city of Modena resides in the Po Valley, marked by extensive urban areas, agricultural fields, intense breeding, and wide manufacturing districts. The region exhibits a warm temperate subcontinental climate (Köppen–Geiger classification Cfa) (Peel et al., 2007), characterized by hot summers and frequent temperature inversions, particularly in the cold period (Caserini et al., 2017). Prevailing winds, generally weak, follow two main directions: WNW and ESE, aligning with the longitudinal axis of the Po Valley. Anthropogenic emissions, combined with topographic and meteorological conditions, contribute to poor air quality (Costanzini et al., 2018; Johnstone & Dawson, 2010). The Northern Apennines act as a climatological divide between continental Europe to the north and the Mediterranean Basin to the south (Cristofanelli et al., 2018).

Modena Observatory characterizes an urban context due to its location in the city centre. Modena features a hot summer climate with intense droughts in July and August, occasionally interrupted by severe thunderstorms, along with cold and wet winters. The transitional seasons are typically rainy, with peaks in fall (October) and spring (April and May).

2.1.2 | Mount Cimone Observatory

The Cimone Observatory, situated at 2165 m a.s.l. on the highest peak in the Northern Apennines (44°11′37′N, 10°42′00′E, WGS84), serves as a strategic location for the Italian Air Force Meteorological Service. Operational since 1937, this observatory has played and currently plays a crucial role in telecommunications, meteorological forecasting, climatology, and air navigation assistance. Positioned above the Planetary Boundary Layer, in the lower free troposphere, and isolated from anthropogenic activities,

the Cimone Observatory holds significance for studying atmospheric composition, especially in measuring background levels of greenhouse gases (Carbone et al., 2014). It is an active participant in the Global Atmosphere Watch program (Cristofanelli et al., 2019; Galli et al., 2019) of the WMO and is part of the Italian Meteorological Network managed by the Air Force Meteorological Service (SYNOP 16134-Metar LIVC).

The climate of Mt. Cimone is classified as alpine, with minimum temperatures ranging from −22°C in winter to 18°C in summer (Colombo et al., 2000; Tositti et al., 2014). Prevailing wind directions include SW and NE, with speeds reaching intensities of 216 $km \cdot h^{-1}$, resulting in a perceived wind chill temperature as low as −45°C (Ciattaglia et al., 2010). Mt. Cimone experiences two rainfall peaks, with the maximum occurring in November and a secondary peak in April.

2.1.3 | Synoptic patterns of the two stations

From a meteorological standpoint, the synoptic weather patterns in Modena and Mt. Cimone exhibit significant similarities, but with some notable exceptions. Instances of heavy rainfall in both locations can occur when a low-pressure system is situated above the Tyrrhenian Sea. Winter cold air flows lead to snowy precipitation in both locations. Strong winds, particularly from the southwest, affect Mt. Cimone. Under these conditions, the Tyrrhenian side of the Apennines experiences cloudiness due to the Stau effect, while Modena may experience the Föhn phenomenon. During intense southwest flows, heavy precipitation has been observed as a result of the spillover effect even at distances 10–20 km downwind from the ridge (Lombroso & Fazlagic, 2000).

In both locations, the influence of large high-pressure fields fosters stable weather conditions. Summer heat waves are driven by the presence of a strong African anticyclone, which causes very high temperatures in both locations, that is, in June, July, and August 2003, August 2017, and June 2019. However, summer in Mt. Cimone is also characterized by convective systems, in some cases with orographic storms (Frontero & Lombroso, 1988).

Stable conditions lead to robust thermal inversions during winter in Modena, resulting in lower temperatures compared to Mt. Cimone. During winter, the phenomenon of thermal inversion is frequently observed, resulting in notable differences between the two stations. This aspect will be further explored in this paper to enhance our understanding of the temperature series and trends calculations.

2.2 | Dataset

For this study, the primary datasets comprise daily historical temperature records, encompassing TX and TN values from 1951 to 2018. The DTR series was also derived to provide a comprehensive perspective.

The Modena Observatory has daily temperature data available from 1861 to the present. To ensure data consistency, the homogenization process was applied to daily TX and TN, following a method by Boccolari and Malmusi (2013). This method underwent some revisions to minimize undocumented corrections made to the original series. In the original study covering 1861 to 2010, homogenization was performed using statistical tests (SNH, Pettitt, Buishand, and Von Neumann) on mDTR (annual average of DTR) and vDTR (annual average of absolute day-to-day differences of the DTR) series (Wijngaard et al., 2003). These tests assess the statistical significance of temperature series homogeneity and identify breakpoints (apart from the Von Neumann test). Corrections, whether documented or not, aim to adjust the series for homogeneity. Notably, more corrections were needed after 1900 compared to the initial 40 years. Evaluation of the first 40 years is challenging due to extensive documented interventions on measuring instruments. Although mathematically homogeneous, corrections in this period may not convincingly show consistent trends. Subsequent corrections for the 1901–2020 period, using the same methodology, yielded a satisfactory outcome. Only two corrections were needed over the 120-year period, passing all four statistical tests at a 0.01 significance level, specifically for the mDTR series. The rejection of vDTR is not surprising, given its relation to the daily variability of temperature. The corrections made symmetrically on TN and TX were as follows:

- Until July 31, 1967 [TX + 0.3°C] and [TN − 0.3°C]; a documented correction corresponding to the calibration of the maxima and minima thermometer.
- Until December 31, 1953 [TX + 0.15°C] and [TN − 0.15°C]; an undocumented correction.

Comparing such new TX and TN trends with those obtained with the previous homogenization by Boccolari and Malmusi (2013), differences of only a few hundredths of a Celsius degree per decade were recorded. Therefore, the results presented in that paper can still be considered valid.

As for the Cimone Observatory, meteorological observations began in 1947 but became systematic only since 1951. The TX and TN series for this observatory were extracted from the European Climate Assessment and

Dataset (ECA&D) platform (Klein Tank et al., 2002). This dataset includes homogenized series derived from data collected by climatological divisions of the National Meteorological and Hydrological Services, observatories, and research centres across Europe and the Mediterranean.

The available TX and TN series include data from January 1, 1951 to December 31, 2020. Notably, there are missing data in the two series, accounting for 352 days for TX and 333 for TN. To address this, a control procedure was applied (Desiato et al., 2012; Dufek et al., 2008) to discard years with more than 30% missing data (i.e., 2019 and 2020 with 63% and 68%, respectively). Uniformly spread gaps over various years were filled through linear interpolation with the other available data. Additionally, the homogeneity of these series was checked using the same method mentioned above, and no corrections were found to be necessary.

The datasets from Modena Observatory and Cimone Observatory, including the computation of seasonal and annual anomalies for TX, TN, and DTR, are presented in section 4.2.

3 | METHODOLOGY

The methodology applied in this study starts from the examination of TX and TN series recorded by both stations spanning from 1951 to 2018. Initially, computations were made for seasonal and annual temperature anomalies, utilizing cross-correlation techniques to identify shared tendencies between the two stations. An analysis about thermal inversions frequency for Modena Observatory has been also included in this section to help the assessment of the differences achieved in winter between the two stations.

Subsequently, an iterative procedure that systematically computed trends and their statistical significance across various periods was employed to partition the time series into meaningful subperiods. Then trends over TX and TN are evaluated, and extreme climate indices from ETCCDI are calculated. The tendencies of these indices and their significance were assessed to elucidate the nuanced changes observed in both stations.

Finally, the UHI contribution has been evaluated using the Urban Minus Rural method (Bian et al., 2014; Manalo et al., 2022; Park et al., 2017; Wu et al., 2019; Zhong et al., 2023), to assess the contribution of urbanization on temperatures and ETCCDI indices trends.

3.1 | Occurrence of daytime temperature inversions in Modena

The Po Valley, where the Modena Observatory is situated, experiences limited ventilation due to its morphology. During the winter, also a weak radiative forcing occurs, contributing to the persistence of stagnant events characterized by the phenomenon of thermal inversions (Caserini et al., 2017) in these situations, lower temperatures can be recorded in Modena compared to Mt. Cimone.

To gain deeper insights into these conditions, an analysis of the seasonal frequency of thermal inversions in Modena was conducted, utilizing data from both observatories. For each day, the lapse rate in°C/100 m was calculated, representing the difference between the temperatures at Mt. Cimone and Modena. This calculation included minimum, maximum, and mean temperatures for every day from 1951 to 2018.

We started examining periods where strong stagnant events have been documented, as during January 1989 and 1990, February 1993, November 1994, January 2012, December 2013, 2015 and 2016, etc. Although thermal inversions typically cease at 1000–1500 m, during these events minimal temperature differences between Modena and Cimone have been recorded. In these periods, the presence of thermal inversions has also been assessed observing radiosonde data. Based on these findings, two thresholds have been selected to identify the presence of thermal inversion in Modena. Aggregating data from all available days across all 12 months spanning from 1951 to 2018, the frequencies of different lapse rate were computed, taking into account the seasonal distribution. Frequency are reported grouped for meteorological seasons, as:

- Winter (DJF): months of December, January, and February.
- Spring (MAM): months of March, April, and May.
- Summer (JJA): months of June, July, and August.
- Fall (SON): months of September, October, and November.

Note that winter season includes the months of December, January, and February. We consider the month of December of 1 year and the January–February of the following year, comprising one winter season.

The results of this analysis, useful for the assessment of differences in temperature anomalies between the two sites (and subsequent trends), are reported in section 4.1.

3.2 | TX and TN anomalies and DTR

Daily series of TX and TN temperatures from 1951 to 2018 for both stations were used to compute daily anomalies. This was done by subtracting the climatological mean for each specific date from the daily values of each series. The climatological mean was based on the Climatic Normal (CLINO) for the period from 1961 to 1990, as defined by the World Meteorological

Organization (WMO) as the standard reference period for long-term climate change assessments. To smooth out large variations due to insufficient samples, a 5-day moving window centred on each specific date was used to average the values. The daily anomalies were subsequently grouped by meteorological seasons to better understand temporal variations and differences between the two stations.

A cross-correlation was computed between the series of seasonal and annual TX and TN anomalies of Modena Observatory and Cimone Observatory. Furthermore, the DTR was computed as the difference between daily TX and the TN at both the Modena Observatory and Cimone Observatory. This calculation provides insights into the variation between the highest and lowest temperatures recorded in a single day, offering a more comprehensive perspective on the temperature dynamics at the two stations. The DTR is particularly valuable in discerning differences in temperature increases between minimum and maximum values. The results are presented in section 4.2.

3.3 | Temperature trends

The analysis of trends in time series is essential in the context of climate change as it provides insights into the evolution of a phenomenon over a specific period. Trends TX, TN, and DTR were evaluated within the time series of both Modena and Mt. Cimone. This analysis firstly covered the entire period from 1951 to 2018, and then specific significant periods were selected based on the subsequent analysis. The goal is to pinpoint statistically significant trends, typically at a confidence level of 99%, by dividing the entire observation period in time intervals covering at least 10 years within this range. This exploration was carried out through an automated procedure that systematically computed trends and their statistical significance across various sequentially periods. These periods include, for example: 1951–2018, 1952–2018, 1953–2018, ..., 2009–2018, 1951–2017, 1952–2017, ..., 2008–2017, ..., 1951–1961, 1952–1961, 1951–1960. The procedure reports the results on a diagram called a "shifting trend," indicating the subperiods to consider for trend calculations. To evaluate the presence and significance of trends on temperatures on the periods identified above, the modified Mann–Kendall test (Kendall, 1957; Pohlert, 2023; Wilks, 2019) was applied, while the Theil–Sen method (Sen, 1968) was used to estimate the slope (section 4.3). These methods are widely used in literature to pursue this aim (Alexander et al., 2006; Mallick et al., 2022; Patra & Satpati, 2022).

Indices from the ETCCDI were selected and applied to the temperature series of both stations. These indices including fixed-value thresholds, absolute measures, percentiles, and duration parameters (Alexander et al., 2006; Klein Tank et al., 2009) were employed to analyse the shifts in extreme climate trends. Fixed threshold indices indicate the number of days per year when a certain condition occurred, whereas percentile indices tally the annual days surpassing or falling below a specified percentile threshold.

To compute these indices MATLAB® scripts were developed and applied. For the Modified Mann–Kendall test MATLAB® pre-existing software was retrieved (Aalok, 2023), developed, and applied. Table 1 lists the selected indices. The extreme climate indices were calculated based on the TX and TN time series for both stations, spanning the entire observational period as well as other significant periods identified by the shifting trend analysis. The trends are expressed in days per decade, and their statistical significance at the 99% and 95% confidence levels was determined using the modified Mann–Kendall test. Comprehensive results are presented in section 4.4.

3.4 | UHI contribution

The UHI effect was assessed following the well-known *Urban Minus Rural* method (Bian et al., 2014; Manalo et al., 2022; Park et al., 2017; Wu et al., 2019; Zhong et al., 2023), which evaluated the impact and contribution of urbanization by comparing rural and urban stations.

A search was carried out to identify data availability from other stations near Modena Observatory for the period of interest from 1951 to 2018.

The Meteorological Service of the Air Force and the National Hydrographic and Mareographic Service (SIMN), have historically been associated with the collection of meteorological parameters in Emilia Romagna and on the national territory. In 1994 the Regional Agency for Prevention, Environment, and Energy of Emilia-Romagna (ARPAE) was established and took over the hydrographic service. Unfortunately, during this period, several stations have been dismissed or changed in their locations. Currently, most of the ARPAE stations have only been operational since 2003 and have no continuity with historical stations. Due to this lack of uninterrupted series from meteorological stations, we considered the ERACLITO dataset (Antolini et al., 2016) provided by ARPAE.

ERACLITO is a daily climatic dataset of precipitation and temperatures (minimum and maximum) covering

TABLE 1 The chosen TX and TN indices defined by ETCCDI (Karl et al., 1999; Zhang et al., 2005).

	Category	Acronym	Name	Definition
TX indices	Fixed threshold	ID	Ice days	No. of days per year when TX < 0°C
		SU	Summer days	No. of days per year when TX > 25°C
	Percentiles	TX90p	Warm days	No. of days when TX > 90th percentile referring the CLINO
		TX10p	Cold days	No. of days when TX < 10th percentile referring the CLINO
	Duration	WSDI	Warm spell	No. of days per year with at least 6 consecutive days when TX > 90th percentile
TN indices	Fixed threshold	FD	Frost days	No. of days per year when TN < 0°C
		TR	Tropical nights	No. of days per year when TN > 20°C
	Percentiles	TN90p	Warm nights	No. of days when TN > 90th percentile referring the CLINO
		TN10p	Cold nights	No. of days when TN < 10th percentile referring the CLINO
	Duration	CSDI	Cold spell	No. of days per year with at least 6 consecutive days when TN < 10th percentile

the entire Emilia Romagna region from 1961 to the present. The data are obtained through spatial interpolation on a regular grid based on values recorded by the network of historical meteorological stations. To extract rural temperature series based on the ERACLITO grid, a Google Earth Engine procedure was implemented, analysing land use maps provided by the CORINE (Coordination of Information on the Environment) program of the European Commission (Büttner et al., 2021) during the period of interest 1961–2018.

We opted to examine the entire timeframe, starting from 1961 due to the availability of ERACLITO data, to assess the impact of the UHI on temperature trends. We excluded the subperiod from 1981 to 2018. This decision is rooted in the substantial urbanization observed in the northern part of Italy, notably post-World War II, fueled by the Marshall Plan. The trend of urban development persisted until around the 1990s and subsequently diminished significantly after 2000 (Romano et al., 2020).

Specifically, we compute zonal statistics to identify rural pixels in the neighbourhood of Modena characterized by predominantly rural land use (Classes 2 and 3) from the CLC datasets available on Google Earth Engine, covering the period 1999–2018 (i.e., years 1990, 2000, 2006, 2012, and 2018) with a resolution of 100 m. Among all the ERACLITO pixels with over 95% rural land cover, four pixels were chosen, located near well-known ARPAE monitoring stations (the grid should provide a more robust estimate in this case).

Figure 2 shows the land use map based on the Corine Land Cover dataset, overlaid with the ERACLITO grid. Highlighted pixels represent those chosen as rural pixels. Specifically:

- ER1 (Campogalliano): the percentage of rural land (Agricultural areas + Forests) calculated in 1990, 2000, 2006, 2012, and 2018 remains consistently at 99%.
- ER2 (Soliera) the percentage of rural land calculated in 1990, 2000, 2006, 2012, and 2018 remains consistently at 99%.
- ER3 (Nonantola): The land use percentage in the two "rural" classes is 100% in 1990, 98% in 2000 and 96% for the remaining years.
- ER4 (Castelfranco): the percentage of rural land is consistently 100% in all years.

TN and TX series from selected ERACLITO pixels were undergone to homogeneity checks. TN and TX series of selected ERACLITO pixels were subjected to homogeneity checks using mDTR and vDTR methodology including the SNH, Pettitt, Buishand and Von Neumann tests, as described above used for Modena and Cimone Observatory series. Some significant breaking points have been identified in the ERACLITO series. As potential issues concerning minimum temperatures have been mentioned in the literature (Antolini et al., 2016) corrections have been applied to TN. Modena Observatory, in this case, was retained as the reference urban station.

Temperature and index trends have been also computed for ERACLITO pixels and Modena Observatory for the period 1961–2018 to retrieve the Urbanization Effect (UE) and Urbanization Contribution (UC), defined as

$$\mathrm{UE} = \Delta T_{\mathrm{urban-rural}},$$

$$\mathrm{UC} = \left| \frac{\Delta T_{\mathrm{urban-rural}}}{T_{\mathrm{urban}}} \right| * 100,$$

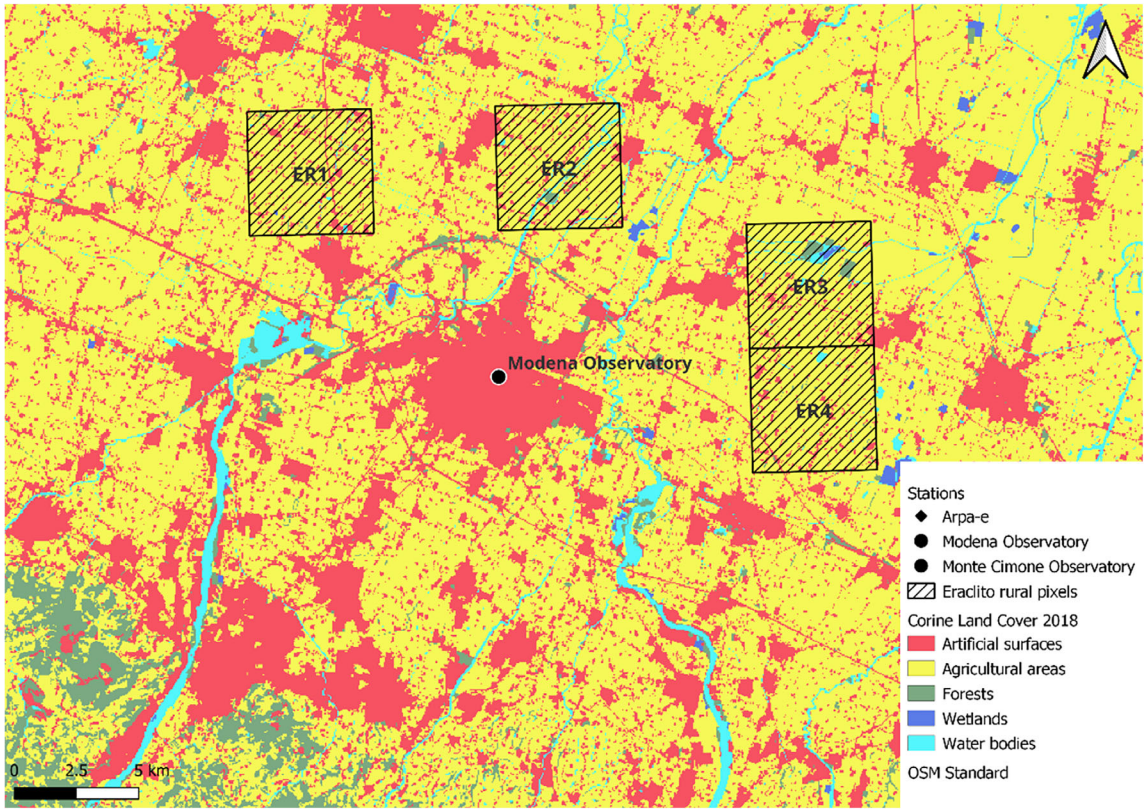

FIGURE 2 Map of land use based on the Corine Land Cover dataset, superimposed with the Eraclito grid. Highlighted pixels indicate selected rural areas: ER1 (Campogalliano), ER2 (Soliera), ER3 (Nonantola), and ER4 (Castelfranco Emilia). [Colour figure can be viewed at wileyonlinelibrary.com]

where T_{urban} is the linear trend of temperature indices in the urban station of Modena Observatory, and T_{rural} is the averaged linear trend of temperature indices in rural stations (ER1, ER2, ER3 and ER4). Results of UHI contributions, together with temperature and indexes trends are reported in section 4.5.

4 | RESULTS AND DISCUSSION

In this section, we present the key findings of our study, delving into the observed patterns and trends to better understand the changes between Modena and Mt. Cimone.

4.1 | Occurrence of daytime temperature inversions in Modena

Through the analysis of documented strong stagnant events that occurred in Modena, also supported by radiosonde data, we identified the thresholds of −0.2°C/100 m and −0.3°C/100 m useful to identify thermal inversions based on the vertical thermal profile calculated between Mt. Cimone and Modena. The thresholds have been defined relating the height of the inversion top with the lapse rate between the two stations. It was observed that the typical height of the inversion top is between approximately 700 and 900 m. The altitude difference between Modena and Cimone is 2131 m, hence cases where the lapse rate between the two stations is 0.0 m or positive are rare since most temperature inversions occur in the lower boundary layer. Typically, a zero or positive lapse rate is observed when the inversion top is high, above 1500 m, an event that is possible but not frequent.

The frequency of intense and persistent thermal inversions, based on the thresholds defined above, grouped by season are reported in Table 2.

Looking at the table, we can observe that the maximum frequency of temperature inversions in Modena occurs in winter, with a more pronounced incidence for minimum temperatures. The frequency is markedly low in spring, nearly absent in summer, and begins to rise again in fall.

4.2 | TX, TN and DTR anomalies

Seasonal and annual anomalies were computed for TX, TN and DTR series of Modena and Mt. Cimone, from

1951 to 2018 with respect to the CLINO base period. The results are presented in Figures 3–6.

All seasonal anomalies consistently exhibit a systematic increasing trend since the late 1990s, which are consistent with previous studies (Brunet et al., 2005; Brunetti et al., 2006; Ciccarelli et al., 2008; Klein Tank et al., 2002; Toreti & Desiato, 2008).

Recent years showed noticeable positive anomalies in both stations, particularly in winter and summer, while they are less evident in intermediate seasons, especially in fall.

In Modena, the peak positive anomalies for TX and TN occurred during the summer of 2003, marked by an intense heatwave, with values of 5.2 and 4.7°C, respectively, compared to the CLINO period. Conversely, the lowest negative anomalies for both TX and TN were recorded in the winter of 1963, with values of −3.4 and −3.3°C, respectively, categorizing it as one of the most severe Extreme Cold Weather (ECW) events in Modena (Lombroso & Quattrocchi, 2008). This aligns with broader European observations during the winter of 1962/1963, documented across Western Europe by 24 stations from Madrid to Rome (Twardosz & Kossowska-Cezak, 2016). Such extreme winters have not recurred since, although the possibility still exists despite the ongoing impact of climate change (Sippel et al., 2024).

For Mt. Cimone, the maximum TX anomaly was observed in the summer of 2017, reaching 4.8°C. This period in Western Europe and the Euro-Mediterranean was notable for extremely hot heatwaves (Otto et al., 2017).

Particularly, an intense heatwave in early August was described as the "worst heatwave since 2003" in southern Europe, with local maximum temperatures in Italy and the Balkans exceeding 40°C for several days. For the Cimone Observatory, a daily TX of 24.0°C was measured on August 3, 2017, marking it the second warmest day in the period 1951–2018. The minimum TX anomaly of −3.2°C was recorded in the fall and winter of 1956. Concerning TN anomalies, the highest value of +4.6°C was observed in the winter of 2016, while the lowest anomaly of −3.2°C was noted in the fall of 1974. It is noteworthy that all maximum anomalies occurred in the 2000s.

TABLE 2 Frequency of thermal inversion grouped for meteorological seasons assuming two different thresholds for their identification: −0.2°C/100 m and −0.3°C/100 m.

	−0.2°C/100 m		−0.3°C/100 m	
	TN (%)	TX (%)	TN (%)	TX (%)
DJF	20.8	18.9	38.3	35.5
MAM	1.0	0.4	3.3	1.3
JJA	0.1	0.0	0.6	0.1
SON	6.2	4.4	13.9	10.2

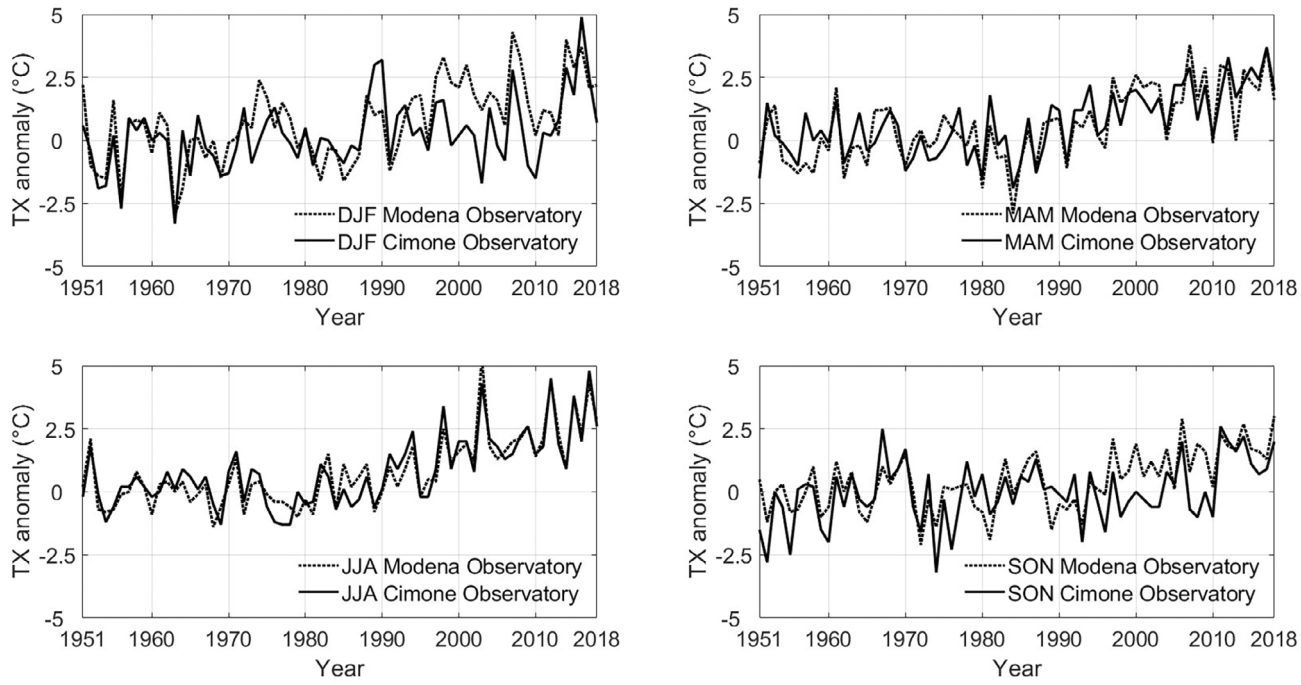

FIGURE 3 Seasonal anomalies of TX for Modena Observatory (·····) and Cimone Observatory (——) calculated with respect to the CLINO 1961–1990.

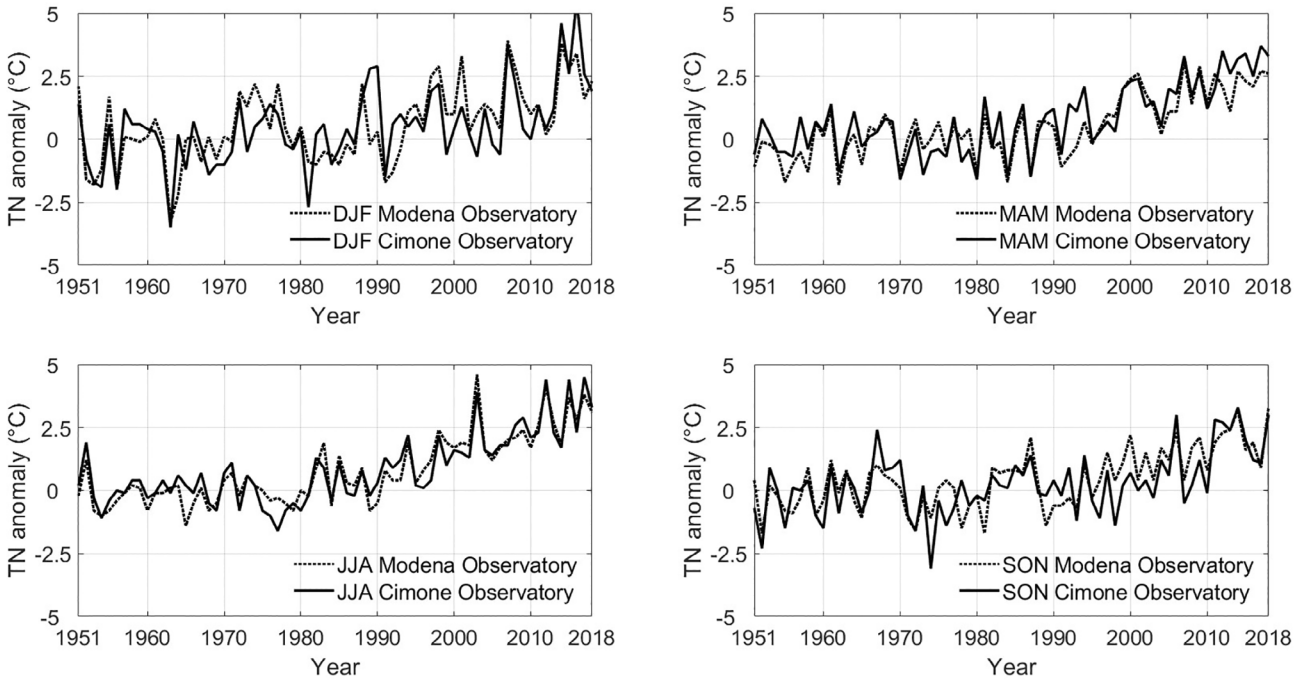

FIGURE 4 Seasonal anomalies of TN for Modena Observatory (·····) and Cimone Observatory (——) calculated with respect to the CLINO base period.

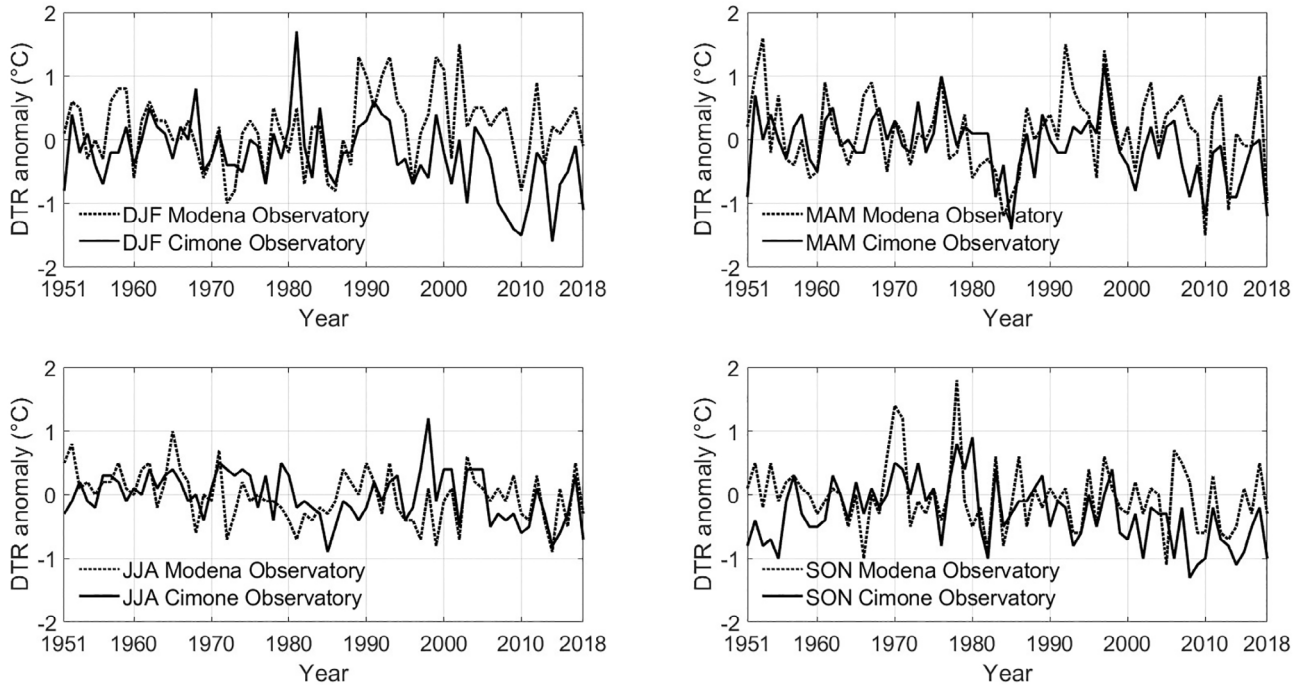

FIGURE 5 Seasonal anomalies of DTR for Modena Observatory (·····) and Cimone Observatory (——) calculated with respect to the CLINO base period.

Concerning DTR, there is a general decrease for all seasons and both stations, attributed to the rise in minimum temperatures compared to maximum temperatures since the late 1990s, as per literature (Bartolini et al., 2008; Brunetti et al., 2000). A noticeable shift between the curves can be observed after the 1990s, particularly during the winter season. The DTR at the Cimone Observatory follows a similar trend to that of the Modena Observatory but with

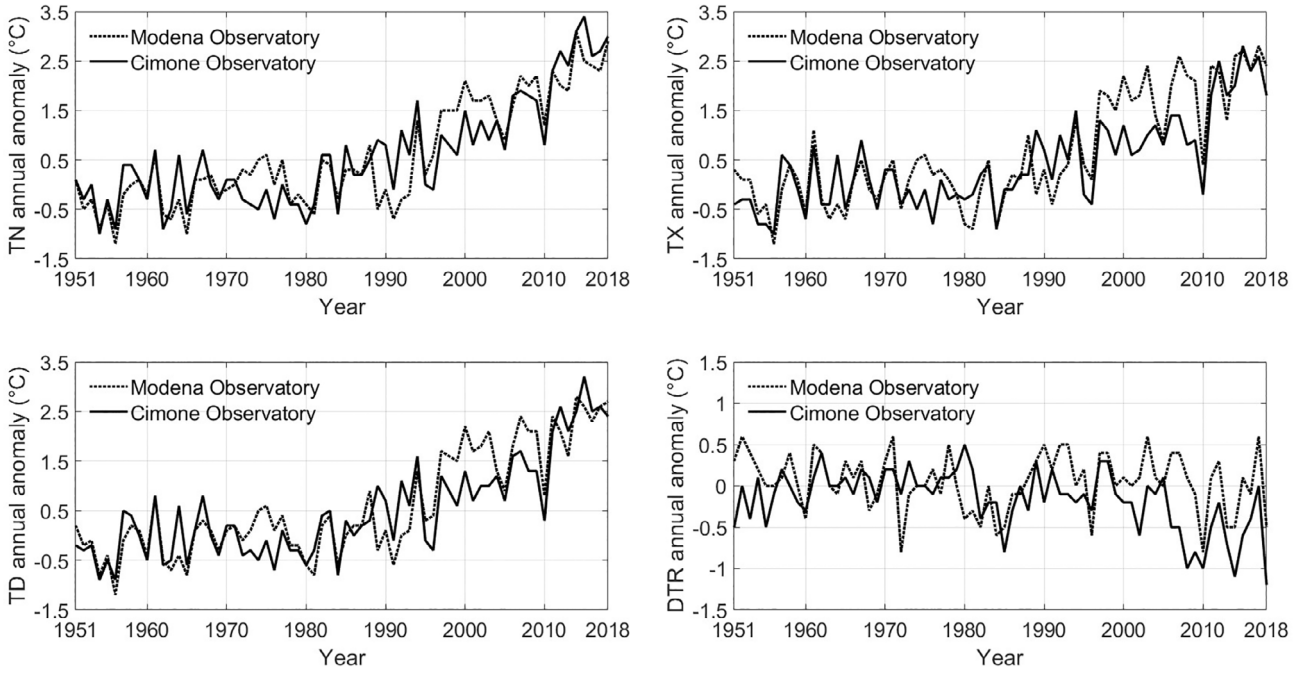

FIGURE 6 Annual anomalies of TN (upper left), TX (upper right), daily average temperature TD (lower left) and DTR for Modena Observatory (·····) and Cimone Observatory (——) with respect to the CLINO base period.

lower difference values. This behaviour is strictly dependent to the increase/decrease trend in TX and TN and has been furthermore analysed in the paper in the subsequent sections.

Concerning annual anomalies, TN shows an increase for both stations after the 1990s. The curves generally follow a similar trend, but they do not appear to be completely correlated. This is also true for TX, although in this case, there is more agreement. From the late 1990s, we noticed a more pronounced increase in TX (but also present in TN) for the Modena Observatory. Naturally, TD's curves, as derived from TN and TX, show a behaviour intermediate between the two. Similarly, the annual DTR seems to have decreased for both stations since the late 1990s, possibly more significantly for the Cimone Observatory. Since the annual anomalies are closely connected to the seasonal ones, the general considerations drawn from the analysis of the above graphs are applicable.

A quantitative analysis was then conducted by computing the correlations between the seasonal and annual time series of anomalies for TX, TN, and DTR at the two stations. Given the relative proximity of the two sites, a high correlation was expected. Table 3 confirms this expectation, showing a high correlation between the indicated parameters with statistical significance and *p*-values lower than 0.01.

Table 3 shows consistent patterns across seasons and the entire year. The weakest correlations were typically observed in winter and fall. Winter, marked by robust thermal inversions impacting the Po Valley and Modena, introduces substantial variations in meteorological conditions between Modena Observatory and Cimone Observatory (see section 4.1). In these situations, Modena experiences low clouds, while Cimone has clear skies, leading to higher maximum temperatures in Mt. Cimone compared to Modena. In contrast, summer sees the influence of a potent African anticyclone, contributing to sunny days and high temperatures in both locations.

Notably, there is a slightly weaker correlation for DTR during JJA with a value of 0.34, suggesting a potential divergence in temperature patterns between the two stations during summer. In fact, Colangelo et al. (2022) found that in this season anticyclonic conditions can lead to variation in DTR (due to night-time temperatures) especially between rural and urban sites.

TABLE 3 Correlation analysis of seasonal and annual anomalies for TX, TN and DTR between Modena Observatory and Cimone Observatory.

	DJF	MAM	JJA	SON	YEAR
TX	0.69	0.84	0.94	0.68	0.85
TN	0.75	0.88	0.93	0.77	0.88
DTR	0.42	0.55	0.34	0.44	0.40

Note: All correlations demonstrate statistical significance with a *p*-value lower than 0.01.

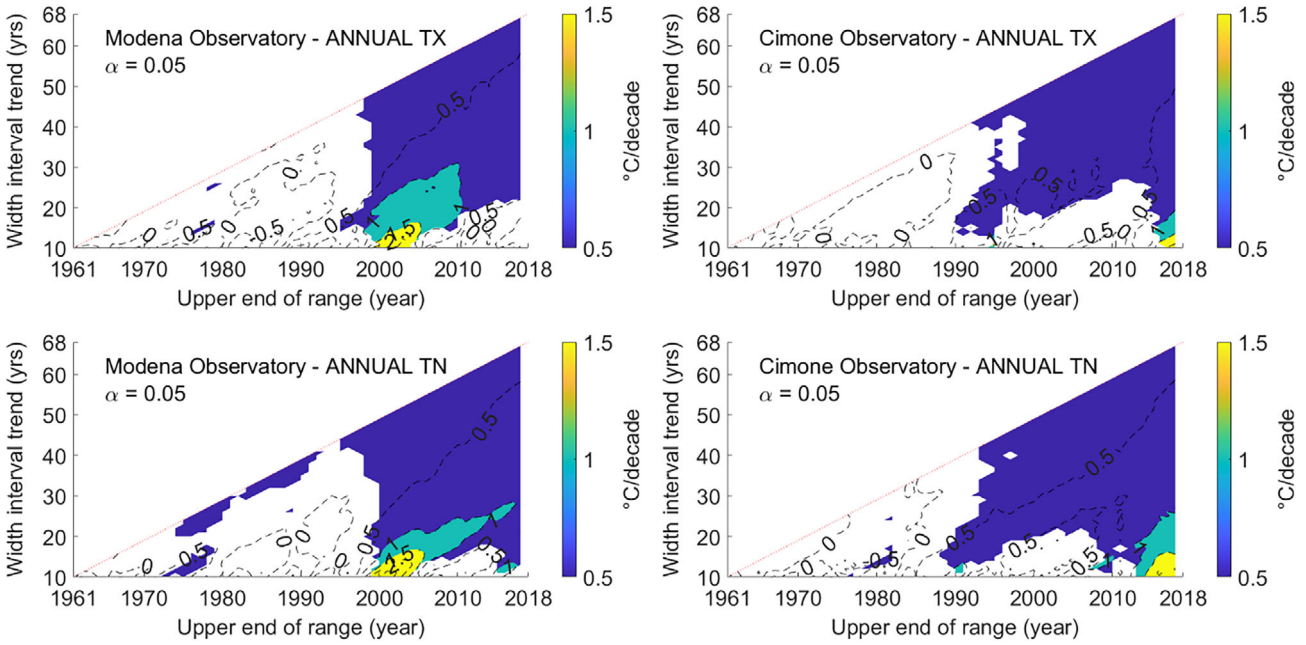

FIGURE 7 Shifting trends calculated from the annual TX (upper line) and TN (bottom line) for Modena Observatory (left column) and Cimone Observatory (right column). Values are expressed in°C·decade^{-1} and if statistically significant at 95% are visualized with a colour palette. [Colour figure can be viewed at wileyonlinelibrary.com]

4.3 | Temperature trends

In this section are reported the results of the analysis carried out on TX, TN, and DTR trends of Modena and Mt. Cimone series. This analysis first covered the entire period from 1951 to 2018, moreover significant periods have been considered based on the shifting trend diagrams reported below.

These diagrams were generated for the annual TX and TN series of both stations, as illustrated in Figure 7. The x-axis denotes the most recent year of each interval, while the y-axis represents the length of the interval. Contour levels indicating 95% statistical significance were visually represented using a colour scale.

For both stations, the statistical significance of the positive trends in the annual TX is observed for intervals lasting at least approximately 20 years, with the upper year of the oldest period falling around the year 2000. TN graphs exhibit a similar pattern to TX.

The retrieved diagrams suggest that the period 1981–2018 is significant for trend analysis, unlike the preceding period of 1951–1980. Shifting trends were also calculated for various seasons, confirming the significance of the 1981–2018 period.

Thus temperature trends and ETCCDI indices will be computed for the entire period from 1951 to 2018 and the significant period from 1981 to 2018. For completeness, calculations were also performed for the period 1951–2018, and the results consistently demonstrated nonsignificant trends, aligning with the anticipated outcome in the shifting trends identification procedure. Scientific literature further supports these findings, affirming that the period from 1951 to 1980 exhibits no significant trends. Wild (Wild, 2013, 2016) highlighted distinct temperature trends in the Northern Hemisphere during this timeframe compared to the subsequent years. Specifically, the data suggests a slight overall cooling in the 1950s to 1980s, followed by a substantial overall warming from the 1980s onward.

Subsequently, trends were assessed for TX, TN and DTR using the data from both stations for the periods 1951–2018 and 1981–2018. The results of the analysis are presented in Table 4.

Concerning TX, the period from 1981 to 2018 reveals heightened temperature trends at the Modena Observatory, registering values up to 0.91°C·decade^{-1} in spring and generally higher for all seasons/entire year except fall. Conversely, Mt. Cimone exhibits high trend values in summer and spring (0.84 and 0.77°C·decade^{-1}). These trends demonstrate statistical significance at the 99% confidence level, excluding winter and fall at Mt. Cimone. Examining the broader period from 1951 to 2018, most seasonal trends achieve statistical significance at the 99% confidence level (with the exception of the fall at Mt. Cimone) and exhibit positive Sen's slopes. Annual trends range from 0.43°C·decade^{-1} (1951–2018) and 0.84°C·decade^{-1} (1981–2018) in Modena to 0.35°C·decade^{-1} (1951–2018) and 0.62°C·decade^{-1} (1981–2018) in Mt. Cimone.

TABLE 4 Seasonal and annual TX, TN and DTR trends (°C·decade^{-1}) for Modena Observatory and Cimone Observatory calculated for the periods 1951–2018 and 1981–2018.

		Modena Observatory			Cimone Observatory		
		TX trend	TN trend	DTR trend	TX trend	TN trend	DTR trend
DJF	1951–2018	0.45*	0.39*	0.03	0.25*	0.35*	−0.10*
	1981–2018	0.88*	0.87*	0.00	0.33**	0.62*	−0.33*
MAM	1951–2018	0.46*	0.45*	0.00	0.41*	0.48*	−0.08*
	1981–2018	0.91*	0.83*	0.08	0.77*	0.92*	−0.11
JJA	1951–2018	0.45*	0.52*	−0.07*	0.41*	0.46*	−0.05**
	1981–2018	0.87*	0.86*	0.00	0.84*	0.88*	−0.04
SON	1951–2018	0.33*	0.37*	−0.04	0.22*	0.30*	−0.08*
	1981–2018	0.68*	0.72*	0.00	0.37**	0.50*	−0.17*
YEAR	1951–2018	0.43*	0.45*	0.00	0.35*	0.42*	−0.08*
	1981–2018	0.84*	0.77*	0.00	0.62*	0.80*	−0.15*

Note: (*) Statistically significant at 99%; (**) statistically significant at 95%.

However, it is noteworthy that the magnitudes of these trends are comparatively lower than those computed for the 1981 to 2018 timeframe (Curci et al., 2021).

TN trends exhibit significance over the entire period from 1951 to 2018, as well as during the subperiod from 1981 to 2018 for both observatories. Trends evaluated in the period 1981–2018 demonstrate particularly high values: in Modena, winter records 0.87°C·decade^{-1}, summer 0.86°C·decade^{-1}, while in Mt. Cimone the maximum value occurs in spring at 0.92°C·decade^{-1}, followed by 0.88°C·decade^{-1} in summer. Trends computed for 1951–2018 exhibit positive slopes, although with lower values compared to the period 1981–2018. Annual trends range from 0.45°C·decade^{-1} (1951–2018) and 0.77°C·decade^{-1} (1981–2018) in Modena to 0.42°C·decade^{-1} (1951–2018) and 0.80°C·decade^{-1} (1981–2018) in Mt. Cimone.

In conclusion, the trends in TX and TN observed during the 1981–2018 period exhibit more pronounced warming compared to those spanning from 1951 to 2018. This trend aligns with established literature (i.e., Acquaotta et al., 2015; Ventura et al., 2002); moreover, studies indicate significant warming trends between 1978 and 2011 (Fioravanti et al., 2016) and a general increase in air temperature post-1980 (Chung et al., 2004; Klein Tank et al., 2002; Türkeş et al., 2016).

Regarding DTR trends, Modena Observatory shows non-significant trends, except for JJA (at 99%) over the entire 1951–2018 period. In contrast, Cimone Observatory consistently exhibits significant negative DTR trends, except for the spring and summer seasons for the period 1981–2018 and the summer season for the period 1951–2018 (but significant at 95%).The values of the DTR in Mt. Cimone are a consequence of the trends computed on TX and TN: TN trends showed in both periods a more pronounced growth with respect to TX trends, resulting in negative DTR trends. This aspect is consistent with other studies found in the literature on mountain stations (Brugnara et al., 2016). Finally, except for DTR, these findings generally corroborate the expectation of similar results between the two stations.

4.4 | Trends of climate indices

The extreme climate indices outlined in Table 1 were calculated based on the TX and TN time series discussed earlier, spanning both the broader period of 1951–2018 and the specific subperiod of 1981–2018. The trend values, expressed in terms of the number of days per decade, are detailed in Table 5 for TX and Table 6 for TN, encompassing both periods and stations. Additionally, the statistical significance, determined through the modified Mann–Kendall trend test at the 99% and 95% confidence levels, is also included.

4.4.1 | Maximum temperature indexes

Careful examination of the ETCCDI indices calculated for TX at Modena Observatory and Cimone Observatory reveals valuable insights into the trends. This detailed analysis allows for specific considerations about how these indices evolve over time, facilitating a comparative assessment between the two stations. Extracting the trend for each index, as outlined in Table 5, enhances understanding and provides a robust basis for drawing

Index	Period	Modena Observatory	Cimone Observatory
ID	1951–2018	−0.35	−6.89
	1981–2018	0.00	−8.67
SU	1951–2018	4.66	N/A
	1981–2018	7.10	N/A
TX90p	1951–2018	14.40	7.20
	1981–2018	27.50	15.0
TX10p	1951–2018	−5.13	−4.62
	1981–2018	−10.0*	−6.67
WSDI	1951–2018	6.67	3.69
	1981–2018	18.10	8.95

Note: All values are statistically significant at 99% except one significant at 95% marked with an asterisk (*).

TABLE 5 Trends values, evaluated with the Sen's slope estimator (no. days·decade^{-1}) for various TX climate extreme indices for the periods 1951–2018 and 1981–2018, for Modena Observatory and Cimone Observatory.

Index	Period	Modena Observatory	Cimone Observatory
FD	1951–2018	−4.62*	−8.55*
	1981–2018	−10.00*	−15.00*
TR	1951–2018	7.42*	N/A
	1981–2018	11.70*	N/A
TN90p	1951–2018	15.60*	10.10*
	1981–2018	29.50*	22.10*
TN10p	1951–2018	−7.69*	−5.38*
	1981–2018	−9.44*	−6.67*
CSDI	1951–2018	−1.71*	−0.41*
	1981–2018	0.00*	0.00

Note: For Cimone Observatory values about TR are not available because a day with TN > 20° has never been observed. (*) Statistically significant at 99%.

TABLE 6 Sen's slope (no. days·decade^{-1}) of some TN climate extreme indices trends for 1951–2018 and 1981–2018 periods for Modena Observatory and Cimone Observatory.

conclusive remarks regarding the observed patterns and their implications.

Ice days (ID)

In Modena, there was an initial decline until the mid-1970s, followed by a slight recovery, and then a second decline after the 1990s. From the 2000s onward, values hovered around zero or near zero, except for a few years around 2010 (specifically, February 2012 and March 2018). On the other hand, Mt. Cimone exhibits a general decrease over time, with an initial negative peak in the 1990s and a more significant drop after 2010 (refer to Figure 8). The so-called "ice days" are declining more rapidly in the mountainous area of Cimone compared to the urban zone of Modena. However, both locations exhibit a clear downward trend, indicative of rising temperatures, especially in the period 1981–2018.

Warm days (TX90p)

The TX90p trend for Modena exhibits fluctuations until the 1990s, followed by a pronounced and rapid increase. Cimone Observatory displays a smoother trend with a noticeable ascent from the 1990s onward (Figure 9).

Cold days (TX10p)

The TX10p trend (Figure 10) in Modena indicates a slight decrease until the late 1990s, followed by a significant drop of approximately 20 days between the 1990s and 2000s, and a second decline after 2012. At Mt. Cimone, there is an initial increase in TX10p from the late 1970s to the early 1980s, succeeded by a more pronounced decrease after 2010.

Warm spells (WSDI)

WSDI is an indicator used to measure the annual frequency of warm spells. Specifically, it quantifies the number of periods in a year that consist of at least six consecutive days where the maximum temperature, TX, remains above its climatological 90th percentile. This index provides valuable insight into the occurrence and intensity of prolonged warm spells, which

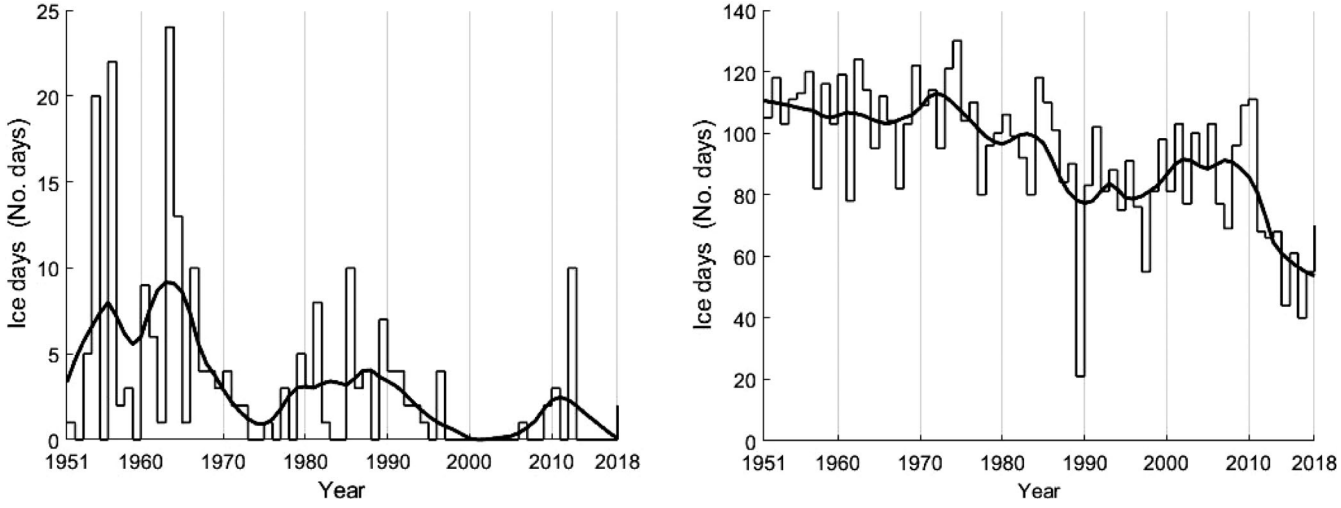

FIGURE 8 Annual series of ID (Ice Days) calculated for Modena Observatory (left) and Cimone Observatory (right), along with a smoothing curve computed using the LOWESS function over an 11-year span.

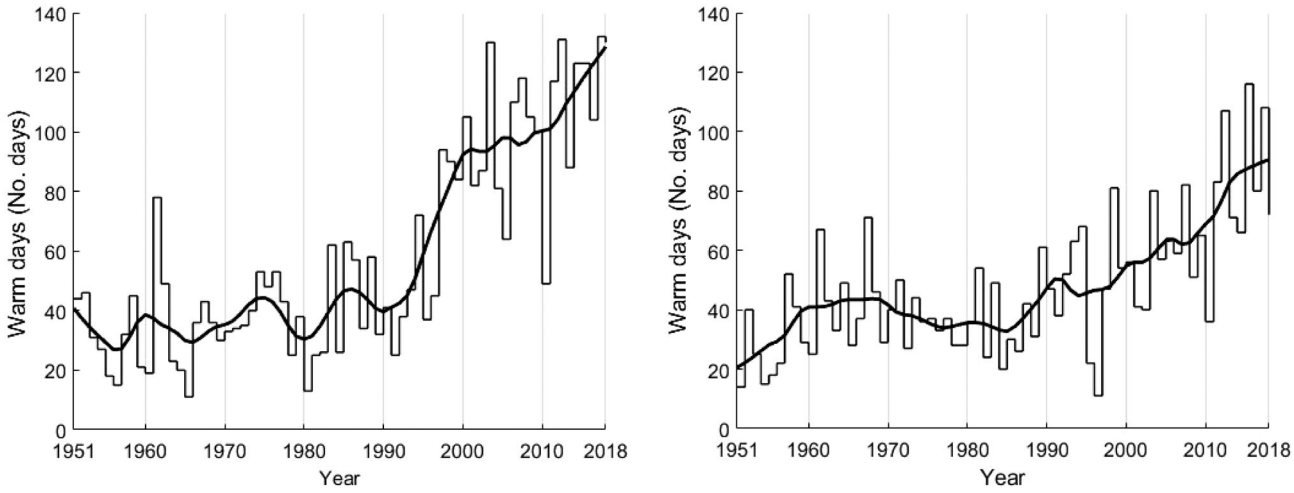

FIGURE 9 Annual series of TX90p calculated for Modena Observatory (left) and Cimone Observatory (right), along with a smoothing curve computed using the LOWESS function over an 11-year span.

are critical for understanding climate change impacts on local and regional scales. In Modena, there has been a significant upswing in WSDI since the early 1990s, indicating a substantial intensification of warm spells. The annual average has surged from approximately 10 days in 1990 to around 60 days at present. Mt. Cimone also exhibits an increase post-1990s, albeit with a less pronounced growth in the number of days compared to Modena (Figure 11).

The "Summer Days" (SU) index is not presented graphically because, for the Cimone Observatory, SU values are not available, given that a day with a TX exceeding 25°C has never been observed. However, these values align with those of other comparable indices, and the 1981–2018 data is nearly double the overall average.

Finally, focusing on TX trends and indices reported in Table 5, several key observations can be made:

- All index trends are statistically significant at a 99% confidence level. Positive trends are observed for SU, TX90p, and WSDI, while negative trends are evident for the others indicating warming.
- Generally, for the periods 1981–2018 and 1951–2018, the warming trend is more pronounced in Modena compared to Mt. Cimone. However, it is important to note that the number of ice days in Modena has reached zero in recent years.

These findings underscore the impact of warming trends, particularly in Modena, as evidenced by various climate indices related to temperature extremes.

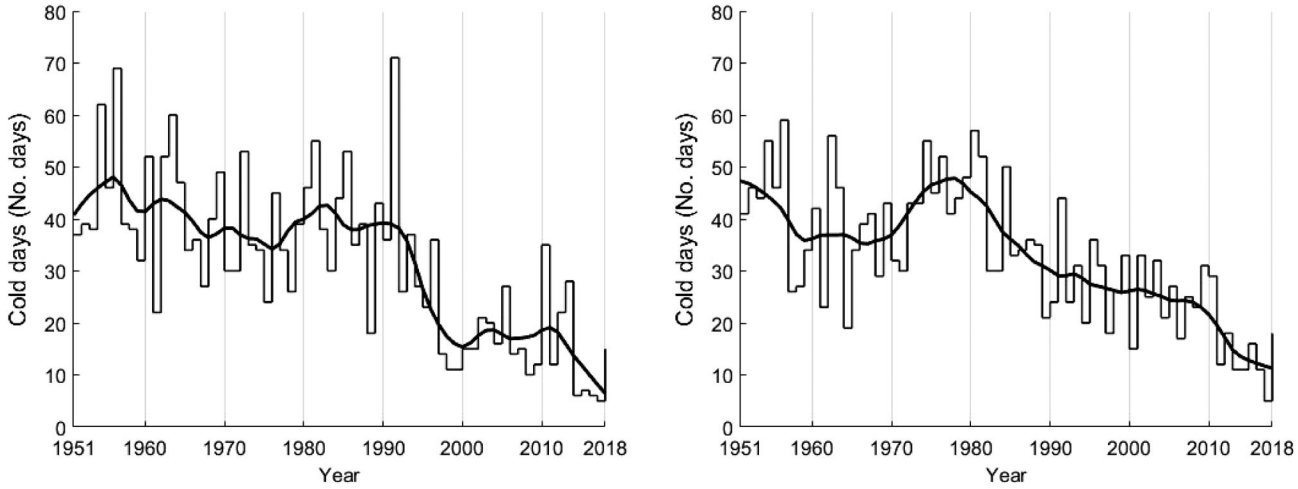

FIGURE 10 Annual series of TX10p calculated for Modena Observatory (left) and Cimone Observatory (right), along with a smoothing curve computed using the LOWESS function over an 11-year span.

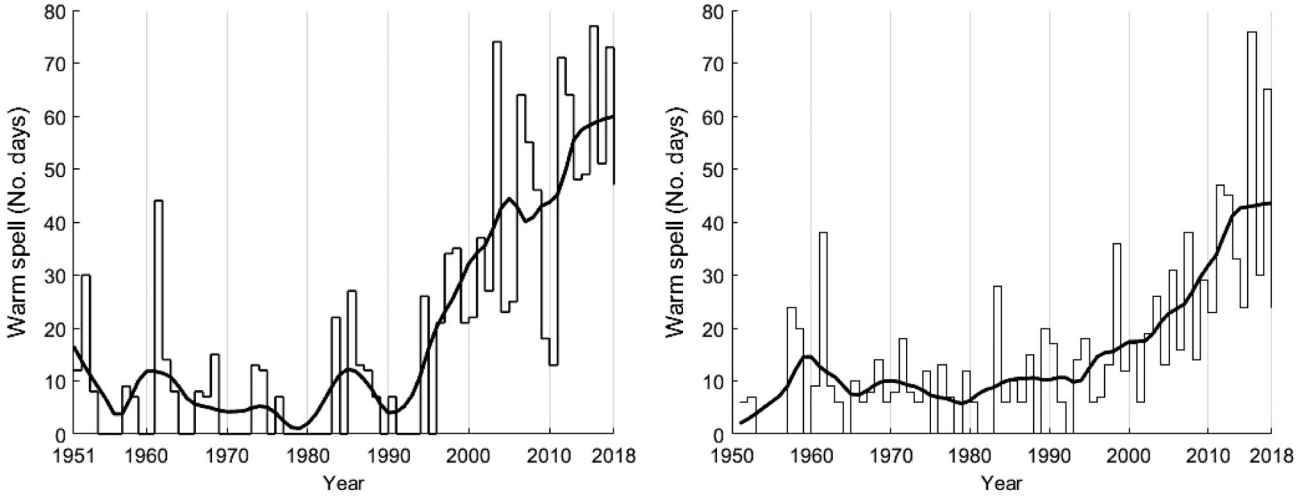

FIGURE 11 Annual series of warm spells calculated for Modena Observatory (left) and Cimone Observatory (right), along with a smoothing curve computed using the LOWESS function over an 11-year span.

4.4.2 | Minimum temperature indexes

Adopting a methodology similar to that used for TX, the ETCCDI indices related to TN and their trends were calculated for the periods 1951–2018 and 1981–2018. The analysis begins with a focus on individual indices, followed by an exploration of trends, as presented in Table 6, and concluding considerations.

Frost days (FD)

Frost days (FD) in Modena exhibit several fluctuations over the years. Notably, a negative peak was observed around the mid-1970s, succeeded by an increase to approximately 40 days per year. Subsequently, a second decline has persisted, with fewer than 10 FD recorded in 2018. The situation for Mt. Cimone is particularly noteworthy, with peak values surpassing 200 days per year in the mid-1970s. A subsequent decrease occurred after the 2000s, followed by a more significant drop after the 2010s. In the late 2010s, the count of frost days is now less than 140 per year (Figure 12).

Warm nights (TN90p)

Concerning TN90p, Figure 13 illustrates a notable upward trend in Modena since 1990, with a more pronounced increase between 1990 and 2000 and from 2010 to 2018. It is noteworthy that the number of warm nights has significantly risen from 40 in 1990 to over 120 in 2018. Mt. Cimone shows a comparable trend to Modena, albeit with a less pronounced increase.

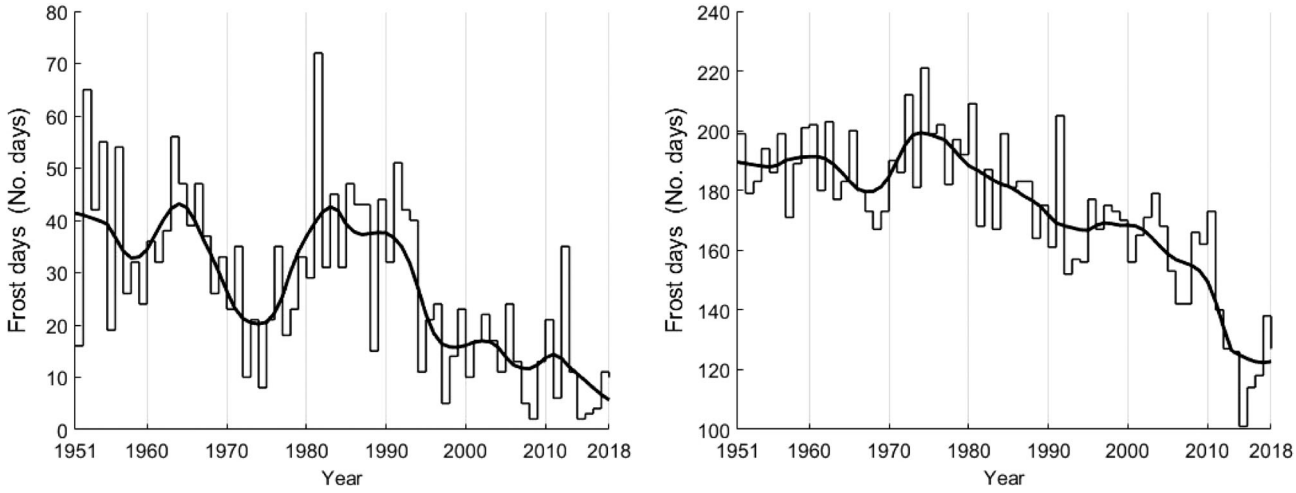

FIGURE 12 Annual series of FD for Modena Observatory (left) and Cimone Observatory (right), along with a smoothing curve computed using the LOWESS function over an 11-year span.

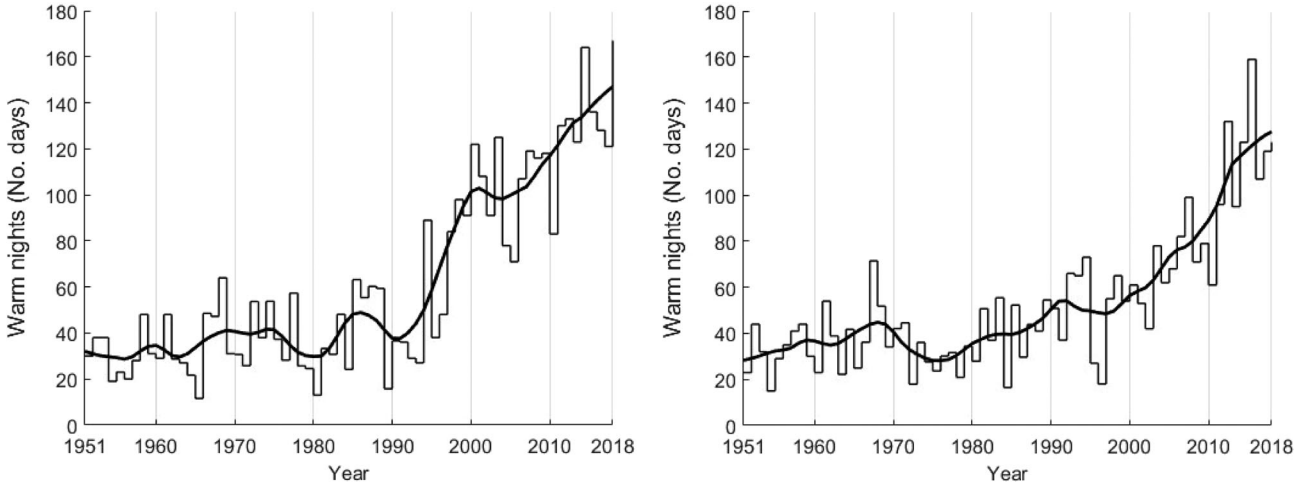

FIGURE 13 Annual series of TN90p for Modena Observatory (left) and Cimone Observatory (right), along with a smoothing curve computed using the LOWESS function over an 11-year span.

Cold nights (TN10p)

TN10p showed a significant decrease since the 1990s, with a plateau observed in the period from 2000 to 2010, followed by a second decrease after 2010. Interestingly, this pattern appears to be specular to that observed for TN90p. In Mt. Cimone, two prominent positive peaks are evident (1951 and the mid-1970s), followed by a general decline towards the end of the studied period (Figure 14).

Cold spells (CSDI)

CSDI is an indicator used to measure the annual frequency of cold spells. Specifically, it quantifies the number of periods in a year that consist of at least six consecutive days where the daily minimum temperature, TN, remains below its climatological 10th percentile. The trends in CSDI for both Modena and Mt. Cimone (Figure 15) closely resemble those observed for TN10p. Since 1990, and a few years later for Modena, there has been a significant reduction in CSDI. After 2000, Modena experienced several instances of zero days, while Mt. Cimone exhibited an exceptional decrease, reaching zero days around the late 2010s.

The TR index has not been calculated for Mt. Cimone because a day with TN >20°C has never been observed. Regardless, they are positive, and as usual, much higher for the 1981–2018 period.

TN indices trends have been computed and are presented in Table 5, offering several notable observations:

- All index trends for both the entire period and the recent period are statistically significant at the 99%

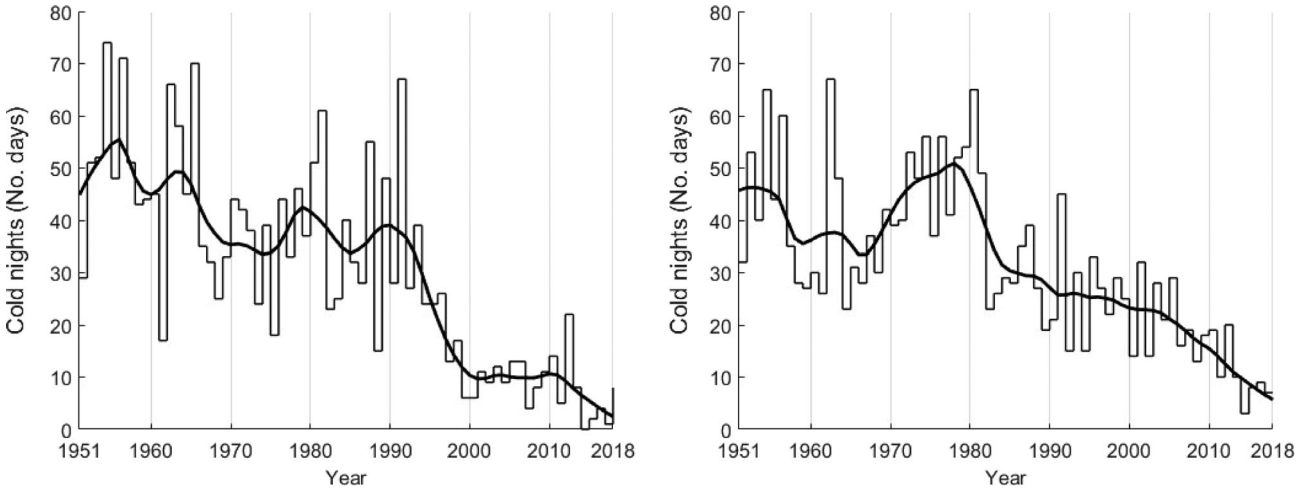

FIGURE 14 Annual series of cold nights calculated for Modena Observatory (left) and Cimone Observatory (right), along with a smoothing curve computed using the LOWESS function over an 11-year span.

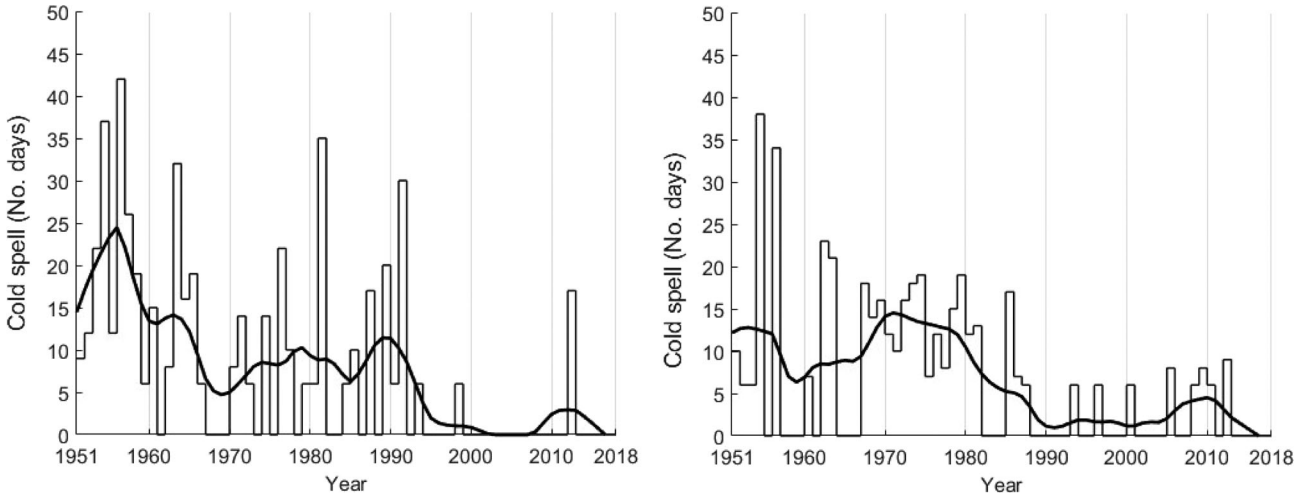

FIGURE 15 Annual series of cold spells calculated for Modena Observatory (left) and Cimone Observatory (right), along with a smoothing curve computed using the LOWESS function over an 11-year span.

confidence level, except for CSDI computed for Cimone Observatory in 1981–2018. Specifically, TR and TN90p show positive trends, while the others exhibit negative trends.

- TN90p and TN10p show a general warming trend more pronounced in Modena than in Mt. Cimone for both periods. This is consistent with the FD trend, where the decrease is more prominent in absolute terms in Mt. Cimone. It is important to note that the number of FD in Modena has reached zero in recent years.

These findings generally align with existing literature evidencing an even-increasing warming. The IPCC AR6 report (Arias et al., 2021; Seneviratne et al., 2021) presents robust evidence for a very likely increase in maximum temperatures and the frequency of heatwaves across Europe. Northern Europe has experienced a significant rise in extreme winter warming events. Additionally, the frequency of winter cold spells has shown a long-term decline in Europe, with the probability of observing cold spell events like those during the 2009–2010 winter being two times smaller than if climate change had not occurred. Furthermore, the IPCC AR5 report (Hartmann et al., 2013) observed across Europe (including the Mediterranean region) the following trends values (expressed in days per decade) in the period 1951–2010:

- TX90p: 4–8 [Modena Observatory 1951–2018: 14.4; Cimone Observatory 1951–2018: 7.20].
- TX10p: −4–0 [Modena Observatory 1951–2018: −5.13; Cimone Observatory 1951–2018: −4.62].

TABLE 7 Seasonal and annual TX and TN trends (°C·decade^{-1}) computed for Modena Observatory (MO) and the ERACLITO pixels (1961–2018).

	MO		ER1		ER2		ER3		ER4		Avg rural	
	TX	TN	TX	TN	TX	TN	TX	TN	TX	TN	TX	TN
DJF	0.53	0.45	0.54	0.53	0.51	0.21*	0.46	0.44	0.43	0.44	0.49	0.41
MAM	0.50	0.50	0.56	0.48	0.38	0.30	0.50	0.38	0.50	0.40	0.49	0.39
JJA	0.55	0.64	0.64	0.50	0.45	0.59	0.67	0.45	0.67	0.53	0.61	0.52
SON	0.39	0.43	0.43	0.50	0.44	0.34	0.37	0.43	0.33	0.44	0.39	0.43
Year	0.52	0.53	0.56	0.50	0.50	0.38	0.51	0.43	0.50	0.45	0.52	0.44

Note: All values are statistically significant at 99%, except for the value marked with an *, significant at 95%.

- TN90p: 4–8 [Modena Observatory 1951–2018: 15.6; Cimone Observatory 1951–2018: 10.1].
- TN10p: −4–0 [Modena Observatory 1951–2018: −7.69; Cimone Observatory 1951–2018: −5.38].

The highest values (in absolute terms) retrieved for Modena and Cimone are also influenced by the last 8 years, excluding from the AR5.

Similar behaviours (increase in TX90p and TN90p, decrease in TX10p and TN10p) have also been identified by Field et al. (2012) for all of Europe and the Mediterranean Region. Concerning our study area, Fioravanti et al. (2013) observed a decreasing trend for FD (up to −8 days·decade^{-1}) from 1961 to 2012 in Mt Cimone.

Finally, the clear pattern emerging from the analysis of extreme indices related to minimum temperatures is a more robust increasing/decreasing trend compared to those of maximum temperatures.

4.5 | UHI contribution

Temperature trends have been computed for Modena Observatory (MO) and selected rural pixels of the ERACLITO grid covering the period 1961–2018, data are reported in Table 7.

Several remarks can be made by observing Table 7. ER3 (Nonantola) and ER4 pixels (Castelfranco Emilia) show similar patterns. This could be related to the closest location of the two pixels, and also because of the interpolation method of the ERACLITO grid explained in the paper of Antolini et al. (2016). ER1 shows higher TX and TN trends compared to the other selected ERs, and ER1 TX trend is even higher than Modena Observatory. ER1, although characterized by 99% agricultural land coverage, is crossed by the highway and surrounded by urban centres. Interesting observations can be made by observing annual TX and TN trends for all considered stations: maximum temperature trends are all very similar, and the highest value belongs to ER1. Minimum temperature trends are lower for rural pixels with respect to MO, especially in ER2 and ER3. This behaviour can also be observed in JJA: here TN of MO is the highest. These statements can provide us with a first indication regarding the possible influence of an Urban Effect produced by the city of Modena which affects particularly TN values.

Going deep, the average contribution of rural pixels (see column Avg rural) has also been reported in Table 8, along with the UE and UC.

Several observations can be derived from examining Table 8:

- Trends regarding minimum temperatures and their associated indices reveal a more pronounced warming tendency for the urban station at the Modena Observatory compared to rural pixels. This behaviour is not true for the indices associated to TX.
- Notably is the trend associated with TR: while there is an average increase of 3.85 no. days·decade^{-1} for rural stations, there is a rise of 9.00 no. days·decade^{-1} for the urban station at the Modena Observatory.
- A substantial annual effect of urbanization (UE) has been observed for TR (+5.16 no. days·decade^{-1}) and for TN90 with 12.67 no. days·decade^{-1}.
- UC associated to TN shows higher values compared to those associated with TX, particularly a remarkable UC calculated for FD (37%), TR (57%), TN90 (65%) and TN10 (39%).

From these findings, we can assert that in our study area, urbanization has had a more significant impact on temperature indices related to TN, while its influence is weaker for temperature indices related to TX. The greater sensitivity of TN than TX to UE has also been documented in the literature for other countries, such as (Liu et al., 2007; Manalo et al., 2022; Park et al., 2017).

TABLE 8 Temperature and indices trends evaluated for selected ERACLITO rural pixels (ER1, ER2, ER3, ER4), their average (Avg rural), for the Modena Observatory (MO) followed by the estimation of the relative Urbanization Effect (UE) and Urbanization Contribution (UC).

	TN	TX	FD	TR	TN90	TN10	CSDI	ID	SU	TX90	TX10	WSDI
ER1	0.50*	0.56*	−2.27**	1.18	4.20*	−3.33**	0.00**	−0.31*	6.41*	20.00*	−4.75*	9.69*
ER2	0.38*	0.50*	−2.58*	6.19*	9.00*	−7.86*	−1.59*	−0.26*	4.76*	13.12*	−9.33*	15.00*
ER3	0.43*	0.51*	−4.86*	1.50*	12.10*	−5.95*	0.00*	−0.48*	6.11*	17.40*	−4.90*	7.50*
ER4	0.45*	0.50*	−1.25	0.74	2.43**	−2.50**	0.00**	−0.48*	6.06*	17.80*	−5.15*	8.41*
Avg rural	0.44	0.52	−3.24	3.85	6.93	−4.91	−0.40	−0.38	5.84	17.08	−6.03	10.15
MO	0.53*	0.52*	−5.12*	9.00*	19.60*	−8.10*	0.00*	−0.45*	6.19*	18.00*	−5.88*	9.55*
UE	0.09	0.00	−1.88	5.16	12.67	−3.19	0.40	−0.07	0.36	0.92	0.15	−0.60
UC (%)	17	0	37	57	65	39	N/A	15	6	5	3	6

Note: The units of UE for TN and TX are (°C·decade^{-1}), while for FD, TR, TN90, TN10, CSDI, ID, SU, TX90, TX10 and WSDI are no. days·decade^{-1}. (*) Statistically significant at 99%; (**) statistically significant at 95%.

There are numerous explanations for why the minimum temperature increases more consistently than the maximum temperature. Roofs and pavements in urban areas possess a high thermal capacity and low albedo, which leads to them absorbing a significant amount of radiation during the day and slowly releasing it at night (Costanzini et al., 2022). Additionally, due to less permeable surfaces, cities experience limited evapotranspiration compared to the countryside. Several authors (Li et al., 2018, 2020; Oke, 1995) have investigated the correlation between UHI and pollutants. On the one hand, downward radiation decreases with increasing particle concentration in the atmosphere, leading to weaker UHI intensity during the day. Thus, regarding maximum temperature, the presence of pollutants near urban stations may lead to a cooling effect. However, the pollution dome could hinder the formation of the nocturnal inversion layer over cities trapping outgoing terrestrial radiation, and inducing warming in the TN (Rohli & Vega, 2017; Zheng et al., 2018).

In the study context, the Po Valley stands out as one of the most polluted areas in Europe, primarily owing to elevated anthropogenic emissions compounded by frequent episodes of stagnant atmospheric conditions. Nevertheless, the long-term trend and variability of atmospheric PM10 concentration in the Po Valley showed a substantial drop after the 2000s (Bigi & Ghermandi, 2014, 2016). Therefore, we hypothesize that in our territory particle air pollution may have a limited impact on the discussed phenomenon, especially in recent years.

To achieve a final overlook, trends evaluated on extreme indexes obtained in this paper have been compared with the values reported by Boccolari and Malmusi (2013). As computation periods do not fully overlap, we compared the results of 1981–2018 with the findings of Boccolari and Malmusi (2013) for 1981–2010. Table 9 shows these comparisons. It must be highlighted that in Boccolari and Malmusi (2013) only statistical significance

TABLE 9 Climate indices trends values reported by Boccolari and Malmusi (2013) for the period 1981–2010, and those work and those obtained for the period 1961–2018.

Index	Period	Modena observatory
ID	1981–2010	−1.4**
	1981–2018	0.00*
SU	1981–2010	6.4
	1981–2018	7.10*
TX90p	1981–2010	7.0**
	1981–2018	27.5*
TX10p	1981–2010	−3.0**
	1981–2018	−10.0*
WSDI	1981–2010	14.1**
	1981–2018	18.1*
FD	1981–2010	−14.1**
	1981–2018	−10.0*
TR	1981–2010	11.2**
	1981–2018	11.7*
TN90p	1981–2010	8.1**
	1981–2018	29.5*
TN10p	1981–2010	−3.8**
	1981–2018	−9.44*
CSDI	1981–2010	−4.8**
	1981–2018	0.00*

Note: Trend are expressed in no. days·decade^{-1}. (*) Statistically significant at 99%; (**) statistically significant at 95%.

at 95% was assessed, furthermore the (unmodified) Mann–Kendall trend test was used.

Looking at the table several observations can be reported. First, the signs of trends are consistent between the two periods (at most they range from 0 to a non-zero value). Then, all indices have statistical significance (99% for the current work, and 95% by Boccolari and Malmusi (2013)), apart from the summer days, SU (6.4°C·decade^{-1}) which do not have statistical significance, but could be due to the use of Mann–Kendall test and not of the modified one.

All the indices evaluated on TX are growing in absolute value, in particular TX10p and TN90p (but the percentiles-based indices are more interesting because they are based on statistical distributions), apart the ice days, ID, which goes from −1.4 to 0.0. Therefore, the effect of global warming seems to have accentuated the values of the TX indices in recent years.

In relation to TN indices, several trends are notable. TR has shown significant growth, TN90p has seen a substantial increase, and TN10p has also risen in absolute terms. Conversely, FD and CSDI have both exhibited decreases in absolute values. The decrease in FD and CSDI negative trends can be attributed to climate extremization, which has stabilized the number of frost days and the duration of cold spells.

5 | CONCLUSIONS

In this study, the analysis focused on the maximum and minimum temperature series of two historical stations in the Po Valley. The first station is located in an urban area, in the centre of Modena, while the second is a station in the lower free atmosphere, the Monte Cimone Observatory. The purpose was to assess the magnitude of climate changes experienced by both stations since the 1950s and to isolate the urban effect due to the presence of extensive residential and industrial areas in the territory by evaluating the UHI effect in Modena.

From the study, we found positive anomalies in both TX and TN series for both stations, with TX displaying slightly higher hotspots. Subsequently, the analysis explores into the trends of maximum and minimum temperature series over different time periods: 1951–2018 and 1981–2018. TX and TN trends in the period 1981–2018 are almost double those computed on the period 1951–2018, confirming the anomalous rise in temperatures in recent years in both sites. We retrieved TX annual temperature trends (1981–2018) reaching 0.84°C·decade^{-1} for Modena and 0.62°C·decade^{-1} for Mt. Cimone while for TN values of 0.77°C·decade^{-1} for Modena and 0.80°C·decade^{-1} for Mt. Cimone.

This general warming trend is reflected in the calculation of extreme climate indices. For instance, warm days (TX90p) in Modena increased by 27.5 days·decade^{-1} in the period 1981–2018, almost twice the increase observed at the Cimone Observatory (15 days·decade^{-1}). Similarly, the rise in warm nights (TN90p) is more pronounced in Modena, with an increase of 29.5 days·decade^{-1} in the period 1981–2018, compared to 22 days·decade^{-1} at the Cimone Observatory. These results have been confirmed also by the comparison between the results of the present paper (in the period 1981–2018) with the findings of a past study focused on Modena in the period 1981–2010.

Building on the findings of Cundari and Colombo (1992), which established that a single station (Cimone Observatory) can serve as a representative for studying long-term temperature changes in the Po Valley, it can be affirmed that this holds true in broad terms. However, when examining temperature trends in Modena, it becomes apparent that retrieving the urban influence reveals notable differences.

This station, located in the city centre, has been subjected to increasing urbanization over the years. The attempt to quantify the UHI effect in terms of Urbanization Effect and Urbanization Contribution using the reference period 1961–2018, as earlier data were not available, reveals that the UHI effect is significant concerning the rise in minimum temperatures, with notably annual UE and UC, respectively: FD −1.88 no. days·decade^{-1} and 37%, TR 5.16 no. days·decade^{-1} and 57%, TN90 12.7 no. days·decade^{-1} and 65%, and TN10 −3.19 no. days·decade^{-1} and 39%. These results align with studies found in the literature.

In conclusion, this research has contributed to characterizing the Po Valley in terms of urban and free atmosphere stations, highlighting how the impact of climate change affects the two sites. During the last period, the increase in trends for minimum temperatures (particularly notable for Mt. Cimone), the negative diurnal temperature range (DTR) trend observed on Mt. Cimone, and the overall assessment of trends on extreme indices (although some are higher in absolute terms for Modena, they require adjustment for Urban Effects) might even indicate a more pronounced warming trend for Mt. Cimone.

These findings underscore the importance of considering diverse local influences in the analysis of regional climate trends and provide a significant foundation for formulating targeted adaptation and mitigation strategies. Future outlooks should include analysing changes in precipitation trends, with a focus on northern Italy's climatic divide, to gain a nuanced understanding of the climatic changes the territory is experiencing.

AUTHOR CONTRIBUTIONS

Sofia Costanzini: Conceptualization; methodology; software; formal analysis; resources; data curation; writing – original draft; writing – review and editing. **Mauro Boccolari:** Conceptualization; methodology; software; formal analysis; resources; data curation; writing – review and editing. **Stephanie Vega Parra:** Software; writing – original draft; writing – review and editing. **Francesca Despini:** Methodology; formal analysis; data curation; writing – review and editing. **Luca Lombroso:** Formal analysis; resources; supervision. **Sergio Teggi:** Supervision.

ACKNOWLEDGEMENTS

The authors would like to express their appreciation to the staff of the CAMM Monte Cimone by Italian Air Force for their collaboration and support in conducting this study, as well as for their contribution to our shared mission of analysing climate change involving both Observatories. We also acknowledge the data providers in the ECA&D project. Open access publishing facilitated by Universita degli Studi di Modena e Reggio Emilia, as part of the Wiley - CRUI-CARE agreement.

DATA AVAILABILITY STATEMENT

The Modena data were provided by the Geophysical Observatory of Modena, University of Modena and Reggio Emilia, Italy (www.ossgeo.unimore.it), and are available upon request from the corresponding author. The Cimone Observatory data are available at https://www.ecad.eu.

ORCID

Sofia Costanzini https://orcid.org/0000-0003-2227-622X
Mauro Boccolari https://orcid.org/0000-0003-1837-5081
Stephanie Vega Parra https://orcid.org/0009-0009-3850-5817
Francesca Despini https://orcid.org/0000-0002-6813-131X
Luca Lombroso https://orcid.org/0009-0006-3547-8508
Sergio Teggi https://orcid.org/0000-0001-7375-0599

REFERENCES

Aalok, A. (2023) *Modified Mann–Kendall test*. GitHub. Available from: https://github.com/atharvaaalok/Modified-MannKendall-Test/releases/tag/v2.0 [Accessed on 10th January 2024]

Acquaotta, F., Fratianni, S. & Garzena, D. (2015) Temperature changes in the North-Western Italian Alps from 1961 to 2010. *Theoretical and Applied Climatology*, 122(3), 619–634. Available from: https://doi.org/10.1007/s00704-014-1316-7

Alemanno, M., Di Diodato, A., Lauria, L. & Santobuono, N. (2014) Environmental measurements at Monte Cimone GAW station. *International Journal of Global Warming*, 6(4), 424–454. Available from: https://doi.org/10.1504/IJGW.2014.066048

Alexander, L.V., Zhang, X., Peterson, T.C., Caesar, J., Gleason, B., Klein Tank, A.M.G. et al. (2006) Global observed changes in daily climate extremes of temperature and precipitation. *Journal of Geophysical Research: Atmospheres*, 111(D5), D05109. Available from: https://doi.org/10.1029/2005JD006290

Antolini, G., Auteri, L., Pavan, V., Tomei, F., Tomozeiu, R. & Marletto, V. (2016) A daily high-resolution gridded climatic data set for Emilia-Romagna, Italy, during 1961–2010. *International Journal of Climatology*, 36(4), 1970–1986. Available from: https://doi.org/10.1002/joc.4473

Arias, P.A., Bellouin, N., Coppola, E., Jones, R.G., Krinner, G., Marotzke, J. et al. (2021) Technical summary. In: Masson-Delmotte, V., Zhai, P., Pirani, A., Connors, S.L., Pean, C., Berger, S. et al. (Eds.) *Climate change 2021: the physical science basis. Contribution of Working Group I to the sixth assessment report of the Intergovernmental Panel on Climate Change*. Cambridge and New York, NY: Cambridge University Press, pp. 33–144.

Barbieri, T., Despini, F. & Teggi, S. (2018) A multi-temporal analyses of land surface temperature using Landsat-8 data and open source software: the case study of Modena, Italy. *Sustainability*, 10(5), 1678. Available from: https://doi.org/10.3390/su10051678

Bartolini, G., Morabito, M., Crisci, A., Grifoni, D., Torrigiani, T., Petralli, M. et al. (2008) Recent trends in Tuscany (Italy) summer temperature and indices of extremes. *International Journal of Climatology*, 28(13), 1751–1760. Available from: https://doi.org/10.1002/joc.1673

Bian, T., Ren, G., Zhang, B. & Zhang, L. (2014) Urbanization effect on long-term trends of extreme temperature indices at Shijiazhuang station, North China. *Theoretical and Applied Climatology*, 115, 407–418. Available from: https://doi.org/10.1007/s00704-014-1127-x

Bigi, A. & Ghermandi, G. (2014) Long-term trend and variability of atmospheric PM_{10} concentration in the Po Valley. *Atmospheric Chemistry and Physics*, 14(10), 4895–4907. Available from: https://doi.org/10.5194/acp-14-4895-2014

Bigi, A. & Ghermandi, G. (2016) Trends and variability of atmospheric $PM_{2.5}$ and $PM_{10-2.5}$ concentration in the Po Valley, Italy. *Atmospheric Chemistry and Physics*, 16(24), 15777–15788. Available from: https://doi.org/10.5194/acp-16-15777-2016

Boccolari, M. & Malmusi, S. (2013) Changes in temperature and precipitation extremes observed in Modena, Italy. *Atmospheric Research*, 122, 16–31. Available from: https://doi.org/10.1016/j.atmosres.2012.10.022

Bonasoni, P., Cristofanelli, P., Calzolari, F., Evangelisti, F., Bonafe, U., Petritoli, A. et al. (2002) *The Mt. Cimone research station*. Paper presented at Workshop on atmospheric research at the Jungfraujoch and in the Alps.

Bonasoni, P., Giovanelli, G., Evangelisti, F., Colombo, T., Santaguida, R., Corazza, E. et al. (1995) Study of ozone transport at Mt. Cimone. In: *Air pollution and visibility measurements*. Munich, Germany: SPIE, pp. 460–467.

Brugnara, Y., Auchmann, R., Brönnimann, S., Bozzo, A., Berro, D.C. & Mercalli, L. (2016) Trends of mean and extreme temperature indices since 1874 at low-elevation sites in the southern Alps. *Journal of Geophysical Research: Atmospheres*, 121(7), 3304–3325. Available from: https://doi.org/10.1002/2015JD024582

Brunet, M., Sigro, J., Saladie, O., Aguilar, E., Jones, P., Moberg, A. et al. (2005) Long-term change in the mean and extreme state of surface air temperature over Spain (1850–2003). *Geophysical Research Abstracts*, 7, 04042.

Brunetti, M., Buffoni, L., Maugeri, M. & Nanni, T. (2000) Trends of minimum and maximum daily temperatures in Italy from 1865 to 1996. *Theoretical and Applied Climatology*, 66(1), 49–60. Available from: https://doi.org/10.1007/s007040070032

Brunetti, M., Maugeri, M., Monti, F. & Nanni, T. (2006) Temperature and precipitation variability in Italy in the last two centuries from homogenised instrumental time series. *International Journal of Climatology*, 26(3), 345–381. Available from: https://doi.org/10.1002/joc.1251

Büttner, G., Kosztra, B., Maucha, G., Pataki, R., Kleeschulte, S., Hazeu, G. et al. (2021) *User manual: Copernicus land monitoring service_corine land cover*. European Environment Agency (EEA). https://land.copernicus.eu/en/technical-library/clc-product-user-manual/@@download/file

Carbone, C., Decesari, S., Paglione, M., Giulianelli, L., Rinaldi, M., Marinoni, A. et al. (2014) 3-year chemical composition of free tropospheric PM1 at the Mt. Cimone GAW global station–South Europe–2165 m asl. *Atmospheric Environment*, 87, 218–227.

Caserini, S., Giani, P., Cacciamani, C., Ozgen, S. & Lonati, G. (2017) Influence of climate change on the frequency of daytime temperature inversions and stagnation events in the Po Valley: historical trend and future projections. *Atmospheric Research*, 184, 15–23. Available from: https://doi.org/10.1016/j.atmosres.2016.09.018

Chervenkov, H. & Slavov, K. (2021) In: Dimov, I. & Fidanova, S. (Eds.) *ETCCDI climate indices for assessment of the recent climate over Southeast Europe*. Cham: Springer, pp. 398–412.

Chung, Y.-S., Yoon, M.-B. & Kim, H.-S. (2004) On climate variations and changes observed in South Korea. *Climatic Change*, 66(1), 151–161. Available from: https://doi.org/10.1023/B:CLIM.0000043141.54763.f8

Ciattaglia, L., Cundari, V. & Colombo, T. (2010) Atmospheric carbon dioxide measurements at Mt. Cimone, Italy: 1979–1983. *Tellus B*, 39, 13–20. Available from: https://doi.org/10.1111/j.1600-0889.1987.tb00266.x

Ciccarelli, N., von Hardenberg, J., Provenzale, A., Ronchi, C., Vargiu, A. & Pelosini, R. (2008) Climate variability in northwestern Italy during the second half of the 20th century. *Global and Planetary Change*, 63(2), 185–195. Available from: https://doi.org/10.1016/j.gloplacha.2008.03.006

Colangelo, G., Sanesi, G., Mariani, L., Parisi, S.G. & Cola, G. (2022) A circulation weather type analysis of urban effects on daily thermal range for Milan (Italy). *Atmosphere*, 13(9), 1529. Available from: https://doi.org/10.3390/atmos13091529

Colombo, T., Santaguida, R., Capasso, A., Calzolari, F., Evangelisti, F. & Bonasoni, P. (2000) Biospheric influence on carbon dioxide measurements in Italy. *Atmospheric Environment*, 34(29), 4963–4969. Available from: https://doi.org/10.1016/S1352-2310(00)00366-6

Costanzini, S., Despini, F., Beltrami, L., Fabbi, S., Muscio, A. & Teggi, S. (2022) Identification of SUHI in urban areas by remote sensing data and mitigation hypothesis through solar reflective materials. *Atmosphere*, 13(1), 70. Available from: https://doi.org/10.3390/atmos13010070

Costanzini, S., Teggi, S., Bigi, A., Ghermandi, G., Filippini, T., Malagoli, C. et al. (2018) Atmospheric dispersion modelling and spatial analysis to evaluate population exposure to pesticides from farming processes. *Atmosphere*, 9(2), 38. Available from: https://doi.org/10.3390/atmos9020038

Cristofanelli, P., Brattich, E., Decesari, S., Landi, T.C., Maione, M., Putero, D. et al. (2018) The "O. Vittori" Observatory at Mt. Cimone: a "lighthouse" for the Mediterranean troposphere. In: Cristofanelli, P., Brattich, E., Decesari, S., Landi, T.C., Maione, M., Putero, D. et al. (Eds.) *High-mountain atmospheric research: the Italian Mt. Cimone WMO/GAW Global Station (2165 m a.s.l.)*. Cham: Springer, pp. 1–14.

Cristofanelli, P., Putero, D., Naitza, L., Marinoni, A., Calzolari, F., Roccato, F. et al. (2019) *The Italian high-altitude atmospheric observation network*. NextData.

Cundari, V. & Colombo, T. (1992) Atmospheric temperature time series analysis at Mt. Cimone Observatory, Italy, 1946–1991. *Il Nuovo Cimento C*, 15(4), 381–390. Available from: https://doi.org/10.1007/BF02511738

Curci, G., Guijarro, J.A., Di Antonio, L., Di Bacco, M., Di Lena, B. & Scorzini, A.R. (2021) Building a local climate reference dataset: application to the Abruzzo region (Central Italy), 1930–2019. *International Journal of Climatology*, 41(8), 4414–4436. Available from: https://doi.org/10.1002/joc.7081

Della-Marta, P.M., Haylock, M.R., Luterbacher, J. & Wanner, H. (2007a) Doubled length of western European summer heat waves since 1880. *Journal of Geophysical Research: Atmospheres*, 112(D15), D15103. Available from: https://doi.org/10.1029/2007JD008510

Della-Marta, P.M., Luterbacher, J., von Weissenfluh, H., Xoplaki, E., Brunet, M. & Wanner, H. (2007b) Summer heat waves over western Europe 1880–2003, their relationship to large-scale forcings and predictability. *Climate Dynamics*, 29(2), 251–275. Available from: https://doi.org/10.1007/s00382-007-0233-1

Desiato, F., Fioravanti, G., Fraschetti, P., Perconti, W. & Piervitali, E. (2012) Elaborazione delle serie temporali per la stima delle tendenze climatiche. In: *Rapporto ISPRA*, Vol. 32. Stato dell'Ambiente. https://www.isprambiente.gov.it/it/pubblicazioni/stato-dellambiente/elaborazioneserietemporaliperlastimadelletendenzedelclima.pdf

Dufek, A.S., Ambrizzi, T. & Da Rocha, R.P. (2008) Are reanalysis data useful for calculating climate indices over South America? *Annals of the New York Academy of Sciences*, 1146(1), 87–104. Available from: https://doi.org/10.1196/annals.1446.010

Field, C.B., Barros, V., Stocker, T.F. & Dahe, Q. (Eds.). (2012) *Managing the risks of extreme events and disasters to advance climate change adaptation: special report of the intergovernmental panel on climate change*. Cambridge: Cambridge University Press.

Fioravanti, G., Piervitali, E. & Desiato, F. (2016) Recent changes of temperature extremes over Italy: an index-based analysis. *Theoretical and Applied Climatology*, 123(3), 473–486. Available from: https://doi.org/10.1007/s00704-014-1362-1

Fioravanti, G., Piervitali, E., Desiato, F., Perconti, W. & Fraschetti, P. (2013) *Variazione e tendenze degli estremi di temperatura e precipitazione in Italia*. Rome, Italy: Istituto Superiore per la Protezione e la Ricerca Ambientale-ISPRA.

Fratticioli, C., Trisolino, P., Maione, M., Calzolari, F., Calidonna, C., Biron, D. et al. (2023) Continuous atmospheric

in-situ measurements of the CH4/CO ratio at the Mt. Cimone station (Italy, 2165 m a.s.l.) and their possible use for estimating regional CH4 emissions. *Environmental Research*, 232, 116343. Available from: https://doi.org/10.1016/j.envres.2023.116343

Frontero, P. & Lombroso, L. (1988) *Analisi sulle diverse frequenze temporalesche in Appennino e nelle Prealpi*. Paper presented at Atti Della Conferenza Internazionale Di Meteorologia Alpina., 20 Congresso Internazionale di Meteorologia alpina (CIMA 88) Sestola (MO), September 18–25, 1988.

Galli, M., Caracciolo di Torchiarolo, L., Proietti, A. & Lauria, L. (2019) Il C.A.M.M. di Monte Cimone Stazione - Stazione Globale del programma Global Atmosphere Watch dell'Organizzazione Meteorologica Mondiale. *Revista di Meteorologia Aeronautica*, 2, 8–28. Available from: https://www.aeronautica.difesa.it/wp-content/uploads/2023/02/RIVISTA_4_2019.pdf

Hartmann, D.L., Klein Tank, A.M.G., Rusticucci, M., Alexander, L.V., Brönnimann, S., Charabi, Y.A.R. et al. (2013) Observations: atmosphere and surface. In: *Climate change 2013: the physical science basis. Contribution of Working Group I to the fifth assessment report of the Intergovernmental Panel on Climate Change*. Cambridge: Cambridge University Press, pp. 160–254.

Johnstone, J.A. & Dawson, T.E. (2010) Climatic context and ecological implications of summer fog decline in the coast redwood region. *Proceedings of the National Academy of Sciences of the United States of America*, 107(10), 4533–4538. Available from: https://doi.org/10.1073/pnas.0915062107

Kang, K.K., Lee, D.S., Hwang, S.H. & Kim, B.S. (2014) Analysis of extreme weather characteristics change in the Gangwon Province using ETCCDI indices. *Journal of Korea Water Resources Association*, 47(12), 1107–1119. Available from: https://doi.org/10.3741/JKWRA.2014.47.12.1107

Karl, T., Nicholls, N. & Ghazi, A. (1999) CLIVAR/GCOS/WMO workshop on indices and indicators for climate extremes. *Weather and Climate Extremes*, 42, 3–7.

Kendall, M.G. (1957) Review of rank correlation methods. *Biometrika*, 44(1–2), 298. Available from: https://doi.org/10.2307/2333282

Klein Tank, A.M.G., Können, G.P. & Selten, F.M. (2005) Signals of anthropogenic influence on European warming as seen in the trend patterns of daily temperature variance. *International Journal of Climatology*, 25(1), 1–16. Available from: https://doi.org/10.1002/joc.1087

Klein Tank, A.M.G., Wijngaard, J.B., Können, G.P., Böhm, R., Demarée, G., Gocheva, A. et al. (2002) Daily dataset of 20th-century surface air temperature and precipitation series for the European climate assessment. *International Journal of Climatology*, 22(12), 1441–1453. Available from: https://doi.org/10.1002/joc.773

Klein Tank, A.M.G., Zwiers, F.W. & Zhang, X. (2009) *Guidelines on analysis of extremes in a changing climate in support of informed decisions for adaptation. Climate data and monitoring*. Geneva: WMO. WMO/TD-No. 1500.

Li, H., Meier, F., Lee, X., Chakraborty, T., Liu, J., Schaap, M. et al. (2018) Interaction between urban heat Island and urban pollution Island during summer in Berlin. *Science of the Total Environment*, 636, 818–828. Available from: https://doi.org/10.1016/j.scitotenv.2018.04.254

Li, H., Sodoudi, S., Liu, J. & Tao, W. (2020) Temporal variation of urban aerosol pollution Island and its relationship with urban heat Island. *Atmospheric Research*, 241, 104957. Available from: https://doi.org/10.1016/j.atmosres.2020.104957

Liu, W., Ji, C., Zhong, J., Jiang, X. & Zheng, Z. (2007) Temporal characteristics of the Beijing urban heat Island. *Theoretical and Applied Climatology*, 87(1), 213–221. Available from: https://doi.org/10.1007/s00704-005-0192-6

Lombroso, L., Costanzini, S., Despini, F. & Teggi, S. (2020) Annuario 2020 dell'Osservatorio Geofisico di Modena. *Atti della Societa dei Naturalisti e Matematici di Modena*, 152, 6–35.

Lombroso, L. & Fazlagic, S. (2000) Analisi delle precipitazioni alluvionali del 6-7novembre 2000. *Atti Della Società Dei Naturalisti e Matematici di Modena*, 131, 5–7.

Lombroso, L. & Quattrocchi, S. (2008) L' Osservatorio di Modena: 180 anni di misure meteoclimatiche. Available from: www.libreriauniversitaria.it

Luterbacher, J., Dietrich, D., Xoplaki, E., Grosjean, M. & Wanner, H. (2004) European seasonal and annual temperature variability, trends, and extremes since 1500. *Science*, 303(5663), 1499–1503. Available from: https://doi.org/10.1126/science.1093877

Mallick, J., Islam, A.R.M.T., Ghose, B., Islam, H.M.T., Rana, Y., Hu, Z. et al. (2022) Spatiotemporal trends of temperature extremes in Bangladesh under changing climate using multi-statistical techniques. *Theoretical and Applied Climatology*, 147(1), 307–324. Available from: https://doi.org/10.1007/s00704-021-03828-1

Manalo, J., Matsumoto, J., Takahashi, H., Villafuerte, M., II, Olaguera, L.M., Ren, G. et al. (2022) The effect of urbanization on temperature indices in The Philippines. *International Journal of Climatology*, 42, 850–867. Available from: https://doi.org/10.1002/joc.7276

Meehl, G.A., Karl, T., Easterling, D.R., Changnon, S., Pielke, R., Changnon, D. et al. (2000) An introduction to trends in extreme weather and climate events: observations, socioeconomic impacts, terrestrial ecological impacts, and model projections. *Bulletin of the American Meteorological Society*, 81(3), 413–416. Available from: https://doi.org/10.1175/1520-0477(2000)081<0413:AITTIE>2.3.CO;2

Oke, T.R. (1995) The Heat Island of the urban boundary layer: characteristics, causes and effects. In: Cermak, J.E., Davenport, A.G., Plate, E.J. & Viegas, D.X. (Eds.) *Wind climate in cities*. Dordrecht: Springer, pp. 81–107.

Otto, I., Reckien, D., Reyer, C., Marcus, R., Le Masson, V., Jones, L. et al. (2017) Social vulnerability to climate change: a review of concepts and evidence. *Regional Environmental Change*, 17, 1651–1662. Available from: https://doi.org/10.1007/s10113-017-1105-9

Park, B., Kim, Y., Min, S., Kim, M., Choi, Y., Boo, K. et al. (2017) Long-term warming trends in Korea and contribution of urbanization: an updated assessment. *Journal of Geophysical Research: Atmospheres*, 122(20), 10637–10654. Available from: https://doi.org/10.1002/2017JD027167

Patra, P. & Satpati, L. (2022) Characteristics and trend analysis of absolute and relative temperature extremes indices and related indices of Kolkata. *Theoretical and Applied Climatology*, 148(3),

943–954. Available from: https://doi.org/10.1007/s00704-022-03975-z

Peel, M.C., Finlayson, B.L. & McMahon, T.A. (2007) Updated world map of the Köppen-Geiger climate classification. *Hydrology and Earth System Sciences*, 11(5), 1633–1644. Available from: https://doi.org/10.5194/hess-11-1633-2007

Planton, S., Déqué, M., Chauvin, F. & Terray, L. (2008) Expected impacts of climate change on extreme climate events. *Comptes Rendus Geoscience*, 340(9), 564–574. Available from: https://doi.org/10.1016/j.crte.2008.07.009

Pohlert, T. (2023) Non-parametric trend tests and change-point detection. *CC by ND*, 2016(4), 1–18.

Ramponi, V. (2023) Lo sguardo scientifico del monte Cimone. *Clionet*, 7, 187–194. Available from: https://doi.org/10.30682/clionet2307y

Rohli, R.V. & Vega, A.J. (2017) *Climatology*, 4th edition. Burlington, MA: Jones and Bartlett Learning Publishers.

Romano, B., Fiorini, L., Marucci, A. & Zullo, F. (2020) The urbanization run-up in Italy: from a qualitative goal in the boom decades to the present and future unsustainability. *Land*, 9(9), 301.

Scorzini, A.R. & Leopardi, M. (2019) Precipitation and temperature trends over central Italy (Abruzzo region): 1951–2012. *Theoretical and Applied Climatology*, 135(3), 959–977. Available from: https://doi.org/10.1007/s00704-018-2427-3

Sen, P.K. (1968) Estimates of the regression coefficient based on Kendall's tau. *Journal of the American Statistical Association*, 63(324), 1379–1389. Available from: https://doi.org/10.1080/01621459.1968.10480934

Seneviratne, S.I., Zhang, X., Adnan, M., Badi, W., Dereczynski, C., Di Luca, A. et al. (2021) Weather and climate extreme events in a changing climate. In: Masson-Delmotte, V., Zhai, P., Pirani, A., Connors, S.L., Pean, C., Berger, S. et al. (Eds.) *Climate change 2021: the physical science basis. Contribution of Working Group I to the sixth assessment report of the Intergovernmental Panel on Climate Change*. Cambridge and New York, NY: Cambridge University Press, pp. 1513–1766.

Sillmann, J., Kharin, V.V., Zwiers, F.W., Zhang, X. & Bronaugh, D. (2013a) Climate extremes indices in the CMIP5 multimodel ensemble: part 1. Model evaluation in the present climate. *Journal of Geophysical Research: Atmospheres*, 118(4), 1716–1733. Available from: https://doi.org/10.1002/jgrd.50203

Sillmann, J., Kharin, V.V., Zwiers, F.W., Zhang, X. & Bronaugh, D. (2013b) Climate extremes indices in the CMIP5 multimodel ensemble: part 2. Future climate projections. *Journal of Geophysical Research: Atmospheres*, 118(6), 2473–2493. Available from: https://doi.org/10.1002/jgrd.50188

Sippel, S., Barnes, C., Cadiou, C., Fischer, E., Kew, S., Kretschmer, M. et al. (2024). Could an extremely cold central European winter such as 1963 happen again despite climate change? *Weather and Climate Dynamics,* 5(3), 943–957. Available from: https://doi.org/10.5194/wcd-5-943-2024

Stott, P. (2016) How climate change affects extreme weather events. *Science*, 352(6293), 1517–1518. Available from: https://doi.org/10.1126/science.aaf7271

Tomozeiu, R., Pavan, V., Cacciamani, C. & Amici, M. (2006) Observed temperature changes in Emilia-Romagna: mean values and extremes. *Climate Research*, 31(2–3), 217–225.

Toreti, A. & Desiato, F. (2008) Temperature trend over Italy from 1961 to 2004. *Theoretical and Applied Climatology*, 91(1), 51–58. Available from: https://doi.org/10.1007/s00704-006-0289-6

Toreti, A., Desiato, F., Fioravanti, G. & Perconti, W. (2010) Seasonal temperatures over Italy and their relationship with low-frequency atmospheric circulation patterns. *Climatic Change*, 99(1), 211–227. Available from: https://doi.org/10.1007/s10584-009-9640-0

Tositti, L., Brattich, E., Cinelli, G. & Baldacci, D. (2014) 12 years of 7Be and 210Pb in Mt. Cimone, and their correlation with meteorological parameters. *Atmospheric Environment*, 87, 108–122. Available from: https://doi.org/10.1016/j.atmosenv.2014.01.014

Türkeş, M., Yozgatlıgil, C., Batmaz, İ., İyigün, C., Koç, E.K., Fahmi, F.M. et al. (2016) Has the climate been changing in Turkey? Regional climate change signals based on a comparative statistical analysis of two consecutive time periods, 1950–1980 and 1981–2010. *Climate Research*, 70(1), 77–93. Available from: https://doi.org/10.3354/cr01410

Twardosz, R. & Kossowska-Cezak, U. (2016) Exceptionally cold and mild winters in Europe (1951–2010). *Theoretical and Applied Climatology*, 125(1), 399–411. Available from: https://doi.org/10.1007/s00704-015-1524-9

Ventura, F., Rossi Pisa, P. & Ardizzoni, E. (2002) Temperature and precipitation trends in Bologna (Italy) from 1952 to 1999. *Atmospheric Research*, 61(3), 203–214. Available from: https://doi.org/10.1016/S0169-8095(01)00135-1

Wijngaard, J.B., Klein Tank, A.M.G. & Können, G.P. (2003) Homogeneity of 20th century European daily temperature and precipitation series. *International Journal of Climatology*, 23, 679–692. Available from: https://doi.org/10.1002/joc.906

Wild, M. (2013) Relevance of decadal variations in surface radiative fluxes for climate change. *AIP Conference Proceedings*, 1531(1), 728–731. Available from: https://doi.org/10.1063/1.4804873

Wild, M. (2016) Decadal changes in radiative fluxes at land and ocean surfaces and their relevance for global warming. *WIREs Climate Change*, 7(1), 91–107. Available from: https://doi.org/10.1002/wcc.372

Wilks, D.S. (2019) *Statistical methods in the atmospheric sciences*. Amsterdam: Elsevier.

World Meteorological Organization. (2022) *Centennial observing stations: state of recognition report: 2021*. Geneva: WMO.

Wu, Z., Zhang, Q., Song, C., Zhang, F., Zhu, X., Sun, P. et al. (2019) Impacts of urbanization on spatio-temporal variations of temperature over the Pearl River Delta.

Xie, S.-P., Deser, C., Vecchi, G.A., Collins, M., Delworth, T.L., Hall, A. et al. (2015) Towards predictive understanding of regional climate change. *Nature Climate Change*, 5(10), 921–930. Available from: https://doi.org/10.1038/nclimate2689

Zhang, P., Ren, G., Qin, Y., Zhai, Y., Zhai, T., Tysa, S.K. et al. (2021). Urbanization effects on estimates of global trends in mean and extreme air temperature. *Journal of Climate*, 34(5), 1923–1945.

Zhang, X., Hegerl, G., Zwiers, F.W. & Kenyon, J. (2005) Avoiding inhomogeneity in percentile-based indices of temperature extremes. *Journal of Climate*, 18(11), 1641–1651. Available from: https://doi.org/10.1175/JCLI3366.1

Zheng, Z., Ren, G., Wang, H., Dou, J., Gao, Z., Duan, C. et al. (2018) Relationship between fine-particle pollution and the Urban Heat Island in Beijing, China: observational evidence. *Boundary-Layer Meteorology*, 169, 93–113. Available from: https://doi.org/10.1007/s10546-018-0362-6

Zhong, R., Song, S., Zhang, J. & Ye, Z. (2023) Spatial–temporal variation and temperature effect of urbanization in Guangdong Province from 1951 to 2018. *Environment, Development and Sustainability*, 26, 9661–9683. Available from: https://doi.org/10.1007/s10668-023-03113-3

Zullo, F., Fazio, G., Romano, B., Marucci, A. & Fiorini, L. (2019) Effects of urban growth spatial pattern (UGSP) on the land surface temperature (LST): a study in the Po Valley (Italy). *Science of the Total Environment*, 650, 1740–1751. Available from: https://doi.org/10.1016/j.scitotenv.2018.09.331

How to cite this article: Costanzini, S., Boccolari, M., Vega Parra, S., Despini, F., Lombroso, L., & Teggi, S. (2024). A comparative analysis of temperature trends at Modena Geophysical Observatory and Mount Cimone Observatory, Italy. *International Journal of Climatology*, 1–26. https://doi.org/10.1002/joc.8607